Applied Energy 377 (2025) 124396

Contents lists available at ScienceDirect

Applied Energy

journal homepage: www.elsevier.com/locate/apenergy

Evaluating the feasibility of concentrated solar power as a replacement for coal-fired power in China: A comprehensive comparative analysis

Lingxiang Yao [a,b], Zhiwen Guan [a], Yang Wang [a,*], Hongxun Hui [b], Shuyu Luo [a], Chuyun Jia [c], Xingxing You [a], Xianyong Xiao [a]

[a] College of Electrical Engineering, Sichuan University, Chengdu 610044, China
[b] State Key Laboratory of Internet of Things for Smart City and Department of Electrical and Computer Engineering, University of Macau, Macao 999078, China
[c] State Grid Sichuan Electric Power Company, Chengdu 610041, China

HIGHLIGHTS

- Proposing a comprehensive framework to compare CSP and CFP technologies across multiple dimensions.
- Evaluating and comparing CSP and CFP potentials in China using geographical, policy, and economic factors.
- Comparing the potential of hybrid technologies and assessing the benefits of hybrid CSP-PV over standalone CSP.
- Validating the proposed framework with real power station data and conducting sensitivity analysis.

ARTICLE INFO

Keywords:
Concentrated solar power
Coal-fired power
Comparative studies
Techno-economic feasibility
China

ABSTRACT

Concentrated solar power (CSP) is considered one of the promising emerging clean renewable power generation technologies with the potential to replace coal-fired power (CFP). However, the feasibility of CSP as a replacement for CFP has not been systematically and scientifically analyzed, hindering its positioning and future development, and complicating energy transition decision-making by policymakers. To address this issue, this paper proposes a comprehensive framework to thoroughly compare CSP and CFP from multiple perspectives, including industry and technology development status, as well as single and hybrid technology potentials. This framework considers the comprehensive influences of China's geography, policy, and economy, and analyzes land suitability, technical installed capacity and generation capacity, and levelized cost of electricity (LCOE) spatial distribution characteristics from geographical, technical, and economic aspects. Comparative results show that, despite CSP having 2.06 million km^2 available for construction and a generational potential 7.58 to 18.22 times the current national generation, its economically advantageous and technically feasible areas cover only 237,030 km^2 (11.51 % of available land), hindering its widespread adoption as a CFP alternative. To address this, this paper proposes a practical hybrid technology assessment scheme, further comparing promising hybrid CSP-PV and hybrid CFP-Wind systems. Results indicate that hybrid CSP-PV systems increase high-quality regions by 19.79 %, covering 3.5 million km^2 with lower LCOE than hybrid CFP-Wind, marking a 226.19 % increase. The economically advantageous and technically feasible areas exceed 585,020 km^2, a 146.81 % increase compared to standalone CSP. Overall, the study demonstrates that hybrid CSP-PV systems offer significant economic and technical advantages, making them a competitive option for CFP substitution. However, the costs of standalone CSP systems remain considerably higher than those of CFP generation. To improve the feasibility of CSP as a CFP alternative, this paper provides targeted policy recommendations aimed at advancing CSP industry growth, fostering technological innovation, and enhancing market infrastructure.

* Corresponding author.
E-mail address: fwang@scu.edu.cn (Y. Wang).

https://doi.org/10.1016/j.apenergy.2024.124396
Received 27 May 2024; Received in revised form 27 July 2024; Accepted 2 September 2024
Available online 16 September 2024

Nomenclature

Abbreviations

AHP	analytic hierarchy process
CSP	concentrated solar power
CSPP	concentrated solar power plant
CFP	coal-fired power
CFPP	coal-fired power plant
DNI	direct normal irradiance
GIS	geographic information system
LCOE	levelized cost of electricity
NDRC	national development and reform commission
NEA	national energy administration
PV	photovoltaics
TES	thermal energy storage

Symbols

C	cost
E	electricity generation
F	fuel
r	discount rate
OM	operation and maintenance
I	insurance
L	loan
LA	land area
T	tax
η	efficiency

1. Introduction

Since the dawn of the 21st century, rapid societal development has dramatically increased the consumption of non-renewable fossil fuels like coal, leading to a looming energy crisis. Concurrently, excessive greenhouse gas emissions have caused persistent global warming, resulting in rising sea levels, erratic weather patterns, and ecological degradation. In response, the third energy revolution has emerged as a promising solution, garnering extensive global support. Since the signing of the Paris Agreement in 2015, the new energy industry has rapidly expanded, supported by global policies and legislation. By the end of 2023, the global cumulative installed capacity of renewable energy, mainly including solar energy, wind power, and hydropower, reached 3870 GW, accounting for 30.2 % of the global power generation [1], [2]. However, the International Renewable Energy Agency indicates that meeting the 1.5 °C goal set by the Paris Agreement requires more than tripling this installed capacity by 2030, with renewable energy accounting for over 65 % of global power generation [3], necessitating continuous enhancement of new energy installations and accelerated replacement of thermal power [4]. To sum up, although a new energy-driven revolution is on the rise, significant challenges remain on the path to change.

As the world's largest developing country and carbon emitter, China plays a crucial role in global climate governance. In recent years, the continuous promotion of China's "dual carbon" process has significantly increased the proportion of new energy in primary energy consumption, accelerating the substitution of traditional fossil energy. By the end of 2023, China's total installed power generation capacity had reached about 2.92 billion kilowatts, marking a year-on-year increase of 14.07 % [5]. Among them, CFP accounts for 1.39 billion kilowatts, representing 47.62 % of the total [5]. The installed capacity of wind power and solar power are 441 million kilowatts and 609 million kilowatts, respectively, totally accounting for 35.99 %, a 10.86 % increase from the previous year [5], [6]. This indicates that a new energy-dominated power system is gradually taking shape. However, the strong volatility and unpredictability of wind and solar power pose significant challenges to the safety, stability, and economic operation of the power grid. In addition, despite a decline in CFP generation, China's resource endowment of "rich coal, poor oil, and little gas" keeps CFP's generation proportion still over 65 % in recent years [6], [7]. In the short to medium term, CFP will still play a vital role as the "stabilizer" and "ballast" in China's power system. Therefore, finding solutions to solve the contradiction and achieve the coordinated development between "clean and low-carbon" and "safety and stability" is an urgent challenge in China's power system transformation.

In the context of the energy revolution, clean and controllable power generations are particularly valuable throughout the entire low-carbonization process. As an emerging and promising generation technology, CSPP integrates "light-heat-electricity" conversion, large-scale TES, and synchronization characteristics. It can achieve 24-h power generation by integrating TES. Besides, it adopts a steam turbine-synchronous generator like the traditional thermal power plant, which can provide continuous and reliable services such as peak regulation, inertia support, and spinning reserve for power systems [8–12]. Currently, the installed capacity of CSP has reached approximately 7GW by the end of 2023 and is expected to reach 73GW by 2030 [1], [13]. Although the current LCOE of CSP generation is still higher than that of wind and PV generations, the sharp decrease in the LCOE (69 % from 2010 to 2022) indicates that there is still a huge cost reduction potential to be unlocked in the future [14], [15].

As one of two viable solar power generation technologies, CSP generations have been compared with PV generation technologies from the aspects of technology, economy, and environmental impact by many scholars. Quaschning [16] analyzed the impact of annual global irradiance on the costs of PV and CSP generation. The analysis, which included data from 61 sites in Europe and North Africa, found that the break-even irradiance was 1300 kWh/m^2 in 2004 and was predicted to rise to approximately 1600 kWh/m^2 over the next ten years due to greater potential cost reductions in PV systems. Desideri et al. [17] first compared the environmental impact and generation performance of PV and CSP plants using the Life Cycle Assessment method. The study revealed that CSP has a lower environmental impact than PV in terms of CO_2 emissions and energy payback time. Subsequently, Desideri et al. [18] conducted a comparative study to evaluate the performance of CSP plants equipped with TES systems and PV plants. This study explored the feasibility of designing a CSP plant with TES systems for base load operation from a technical perspective without considering in-depth economic analysis. To conduct a comprehensive economic comparison, Hernández-Moro et al. [19] presented a mathematical model for the calculation of the LCOEs for PV and CSPPs. They employed discounted cash flow techniques and the learning curve approach to analyze the future evolution of LCOEs. The study concluded that the LCOE of CSP would decrease substantially from 2010 to 2030, but the rate of cost reduction would slow down significantly thereafter, contrasting with the trend observed in PV. From a more macro perspective, Pietzcker [20] utilize the hybrid energy-economy model REMIND to evaluate and compare the economic potentials of CSP and PV. It was concluded that although PV is initially deployed faster for their lower costs, CSP will catch up and overtake PV at the end of the century due to the lower integration costs of CSP. In [21], Khan et al. reviewed and compared the types, mechanisms, efficiency, and cost factors of PV and CSP technologies. The review indicated that although CSP plant investments are significantly higher, CSP plants yield higher economic returns than PV power plants. Awan et al. [22] conducted a techno-economic comparison of parabolic trough CSPPs and PV plants with the same nameplate capacity in Saudi Arabia. In [23], a similar study is also performed to compare the performances between solar tower CSPPs and PV plants. The two studies show that the CSPPs have much better electrical output compared to PV plants but also with higher LCOEs. Besides, the small-scale dish-Stirling generation technology was also compared with PV generations from both energy and economic perspectives in [24]. The comparative analysis shows that PV systems have a 6.9 % better capacity factor, 54 % more energy output, and nearly one-third the LCOE compared to dish-Stirling generation systems. It can be seen that, despite the high expectations for CSP, the rapid reduction in PV technology costs over the past decade has positioned PV among the most cost-effective renewable energy technologies worldwide. This economic shift has placed CSP at a competitive disadvantage within the global renewable energy market, subsequently impeding its development. As a result, the comparability between CSP and PV technologies has increasingly weakened, leading to a decline in the frequency of comparative research studies between the two technologies.

However, in recent years, with the high penetration of volatile renewable energy sources, the advantages of CSP, notably its consistent output and controllable flexibility, have become increasingly significant. Consequently, maximizing the inherent benefits of CSP has emerged as a primary concern [25]. To this end, from the perspective of dispatchable resources, scholars have conducted comparative analyses of CSP with other forms of power generation, such as nuclear and biomass energy. Chung-Ling et al. [26] compared the costs of CSP with other alternative dispatchable generations, including coal, gas, and nuclear generation. The statistical results showed the competitive viability of CSP generations from both economic and environmental aspects. Pfenninger et al. [27] compared CSP and nuclear from the perspectives of costs, environmental impacts, and possible risks. The results indicated that the CSPPs are smaller investments with lower environmental and financial risks. They could become competitive with nuclear power by 2030 if the costs can be reduced as expected. Li et al. [28] quantitatively compared the roles of CSP and biomass in the spatial and temporal configurations of a 100 % renewable power supply in Australia, focusing on capacity factor and LCOE. Additionally, to fully leverage CSP's dispatchability with low costs, the concept of a hybrid CSP-PV plant has been proposed as a promising and sustainable technology. This hybrid approach combines the complementary strengths of both technologies, potentially offering enhanced grid stability, improved efficiency, and reduced costs. Parrado et al. [29] compared the LCOEs of three 50 MW plants: PV, CSP with 15 h of TES, and a hybrid PV-CSP plant in Chile. The research showed that the hybrid PV-CSP plant is the most reliable and environmentally viable option among the three, even though its LCOE is not the lowest. Starke et al. [30] evaluated the performance of a hybrid CSP-PV plant located in Chile, through parametric analysis and cost optimization. The main results indicated that the hybrid CSP-PV plant, with its optimal LCOE, had a higher capacity factor and lower LCOE compared to the single CSP plant, primarily due to a reduction in the CSP solar field size.

In summary, with the steady advancement of energy transformation and continuous technological innovation, the role of CSP has undergone a significant transformation. Initially functioning as an independent power source, CSP has evolved into a flexible and dispatchable power source, shifting its operational focus from maximizing electricity generation to fully exploiting its energy storage and flexible adjustment capabilities. This evolution allows CSP to offer a sustainable, low-carbon alternative to traditional energy sources like nuclear, geothermal, and coal-fired power. It integrates peak-shaving and energy storage capabilities, enabling the utilization of renewable energy for grid regulation and support. This dual functionality not only provides multi-time-scale power dispatch capabilities but also contributes to the rotational inertia of power systems, positioning CSP as a critical peak-shaving and foundational power source in regions with substantial solar resources. Moreover, hybrid CSP-PV generation technology has been proven to be a cost-effective and technically feasible solution to address the high costs associated with standalone CSP technology. Consequently, in areas like Northwest China, CSP is firmly regarded as a safe and reliable alternative to traditional CFP and an effective means to enhance the consumption of fluctuating renewable energy [9], [25], [31]. Nevertheless, existing research has largely been confined to preliminary case cost analyses and has not conducted a thorough comparative analysis of the feasibility of CSP replacing CFP on a national scale. Moreover, it does not adequately address several key questions: 1) What are the similarities and differences between the development status and technical characteristics of CSP and CFP? 2) Under what conditions or in which regions does CSP currently possess significant potential to replace CFP? 3) How do the potential future technological developments of CSP compare with those of CFP, and what technological trajectory should CSP follow to expedite the replacement of CFP? These gaps underscore the need for more in-depth investigations to better understand CSP's potential as a foundational and peak-shaving power source in specific areas and to fully leverage its capabilities in the transition away from traditional fossil fuels.

In view of the aforementioned, this paper conducts a detailed and in-depth comparative analysis of CSP and CFP, as well as hybrid generation models based on both, from multiple perspectives including industry development status, technological characteristics, and technological potential. The contributions of this study are summarized as follows:

1) A comprehensive framework was proposed to compare CSP and CFP across multiple dimensions, including the industrial and technological development status, and the potential of single and hybrid technologies. This paper assesses the feasibility of replacing CFP with CSP in various regions and explores the potential of hybrid CSP-PV systems for industrial transitions towards sustainable development. To the best of the authors' knowledge, this represents the first extensive comparison between CSP and CFP. The findings offer valuable references for shaping future technological innovation paths and guiding the industrial development of CSP.
2) This paper proposes a comprehensive analysis framework for evaluating the potential of CSP and CFP technologies in China, considering a blend of geographical, policy, and economic factors. This framework integrates GIS data with a multi-criteria decision-making model, a technical potential evaluation model, and the LCOE model. It conducts a comparative analysis from geographical, technical, and economic perspectives, examining the land suitability, technical installed capacity, generation capacity, and spatial distribution of LCOE for both technologies nationwide.
3) From an engineering practice perspective, this paper thoroughly considers the real-world construction scenarios and economic benefits of hybrid power generation, proposing a novel framework for assessing the geographic potential and calculating the LCOE tailored to engineering requirements. The study quantitatively analyzes the geographic and economic advantages of hybrid over single technologies nationwide. It also identifies regions where hybrid CSP-PV systems have both technological and cost advantages over hybrid CFP-Wind systems.
4) This study utilized real power station data to validate the geographic potential results for both single and hybrid power technologies, confirming the reliability of the proposed potential assessment framework. Additionally, a sensitivity analysis is conducted to explore the effects of factors, including generation efficiency, CSP-PV capacity ratios, and industry scaling, on the results. Furthermore, integrating the comparative results with CSP development challenges, this study proposes targeted policy recommendations to advance industry growth, spur technological innovation, and enhance market infrastructure.

The remainder of the paper is structured as follows. Section 2 conducts a comparison of industrial and technological development status between CSP and CFP. Section 3 conducts a comprehensive comparative analysis from three perspectives: geographical, technical, and economic.

Section 4 engages in a comparative analysis of the two hybrid models — the CSP-PV hybrid and the CFP-Wind hybrid. This comparison is conducted from the perspectives of both suitability and LCOE analysis, offering a comprehensive understanding of the relative advantages of each approach. In Section 5, a sensitivity study is conducted, and the corresponding policy suggestion is provided. Section 6 concludes this paper.

2. Comparison of industrial and technological development

2.1. Industrial development status

2.1.1. Installed capacity

Since the 12th Five-Year Plan, China has made significant strides in optimizing its power structure by prioritizing energy transformation and advancing power system reform. As a result, the proportion of clean energy generation has steadily increased. Fig. 1 shows a significant shift in newly installed capacity in China, with solar and wind power generation becoming the mainstay, while CFP has dwindled quickly. Moreover, the proportion of CFP installed capacity has experienced a sharp decline, from 71.48 % in 2012 to 47.62 % in 2023 [7]. Despite CFP generation still accounting for a relatively high proportion, its year-on-year trend has shown a steady decline, from 78.72 % to 69.95 % [7], [32–38]. As a result, CFP is gradually transforming from being the main source of power to a more basic one. This shift facilitates a steady transition towards a low-carbon power system while ensuring the security of the electricity supply.

CSP generation is an emerging technology compared with CFP generation, but it has received extensive attention from the industry and society in recent years due to its huge potential. As shown in Fig. 2, China has made some progress in CSP development, with a cumulative installed capacity of 588 MW by the end of 2023 [39]. However, the overall installed capacity is still insufficient. As of the end of 2023, planned or under-construction CSP projects in Qinghai, Gansu, and Xinjiang exceeded 1 GW each, and there are also project layouts in Inner Mongolia, Jilin, Tibet, and other provinces [39]. The total installed capacity of these projects exceeds 4 GW, and they will go into operation and generate electricity in the next two years [40]. By that time, China's installed capacity of CSP will double. Therefore, experts and scholars in the industry unanimously believe 2022 will mark the beginning of large-scale industrial development of CSP generation in China.

2.1.2. Policy support

To support CSP development, the Chinese government has implemented various targeted policies. In 2005, the NDRC first mentioned CSP generation and recognized it as being in its nascent technological stage [42]. Two years later, the NDRC's "Document No. 2174" proposed demonstration projects totalling 50,000 kW in the northwest region [43]. With support from the "11th Five-Year" 863 Program, Asia's first megawatt-scale experimental CSPP successfully generated electricity in 2012, showcasing China's mastery of core CSP technologies [44], [45]. Subsequently, the NEA issued "Document No. 355" in 2015 [46], opening the construction of the first batch of demonstration projects in China. A year later, the NDRC set the benchmark on-grid demonstration electricity price for CSP generation at 1.15 yuan/kWh, helping the industry surmount its initial hurdles [47]. Although the cancellation of subsidies in early 2020 led to a temporary downturn in the industry, the re-establishment of the subsidy mechanism soon revitalized the CSP sector [48]. By the end of 2020, the installed capacity of these demonstration projects had reached 538 MW, showcasing their peak and frequency regulation capabilities. Additionally, in the past three years, a series of robust policies have been enacted, delineating the direction for the integrated development of CSP, wind power, and PV. Most notably, in April 2023, the NEA issued "Document No. 28," targeting 3 million kilowatts of new CSP construction annually during the "14th Five-Year" period. This policy is expected to significantly accelerate the rapid and large-scale expansion of the CSP industry [49].

The policies for the CSP industry in China are increasingly supportive, while policies for the CFP generation are becoming more restrictive. To achieve carbon emission peak goals, China has implemented targeted policies to control the scale of CFP development and promote its clean transformation. To promote technological advancement and sustainable development in the CFP industry, the new emission standard of air pollutants for CFPPs was released in 2011 [50]. Subsequently, in 2014, Document No. 2093 mandated that new CFP units should be over 600

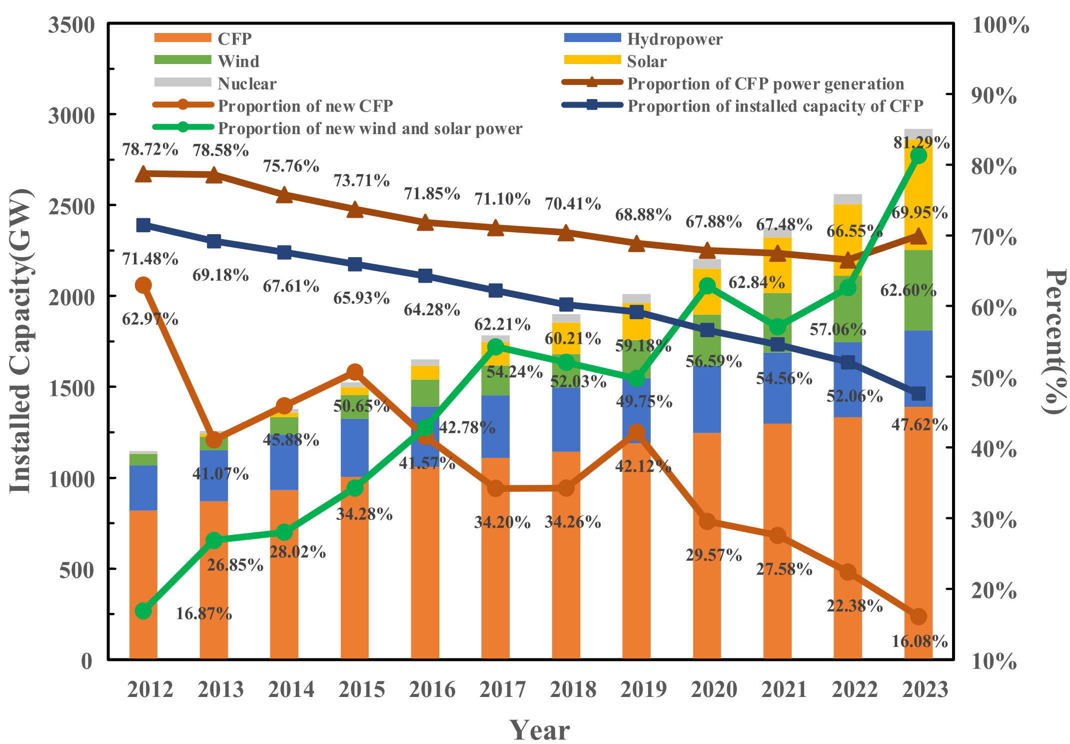

Fig. 1. Proportions of installed capacity, newly installed capacity, and electricity generation [7], [34–38].

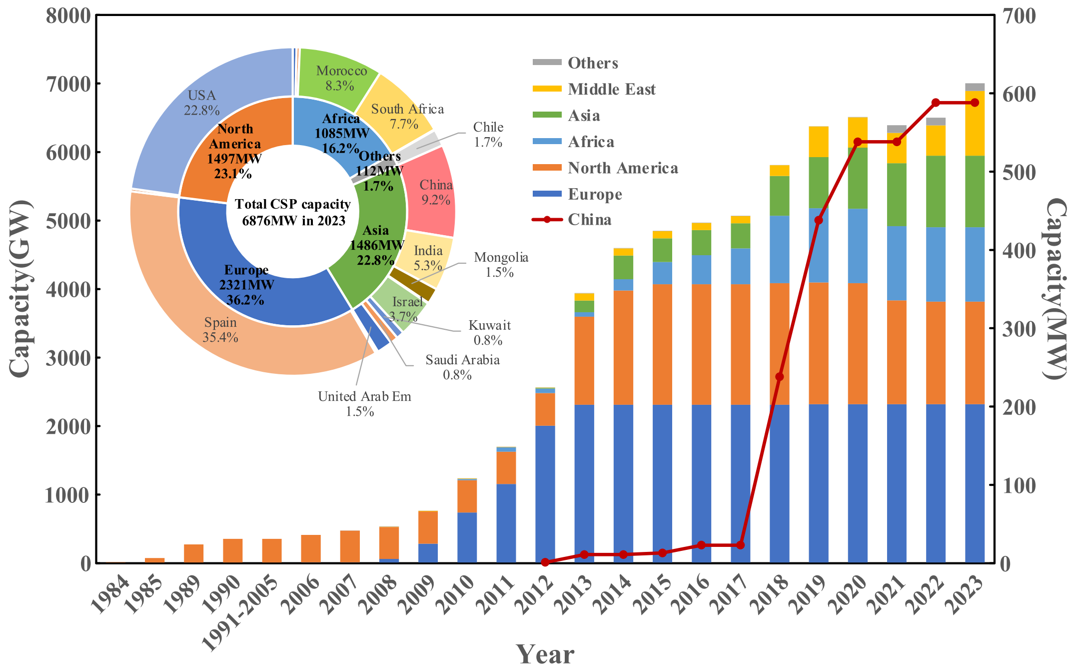

Fig. 2. . Installed capacity of CSP generation [1], [41].

MW and meet gas turbine emission limits [51]. This led to some key projects for ultra-low emission and energy conservation transformation nationwide. In 2015, “Document No. 164” further elevated this to a national action, requiring all capable CFPPs should strive to achieve ultra-low emissions by 2020 [52]. As emission standards increasingly stringent, pressure for cleaner production increased, slowing CFP development. In 2016, the NDRC and NEA issued “Document No. 565”, proposing measures to cancel, postpone approval, and delay construction of CFP projects [53]. In 2022, seven departments jointly issued a document to strictly control CFP projects [54]. Moreover, during the past five years, China also introduced several relevant policies to promote the implementation of CFP unit transformation and upgrading, further reduce CFP unit energy consumption, and enhance their flexibility, regulation capability, and efficient level [55], [56].

Over the past two decades, China has implemented proactive support policies, including price subsidies and research funding, to facilitate the CSP industry’s nascent stage. These initiatives have helped overcome initial barriers, paving the way for significant CSP development. Recent robust support strategies further signal expansive growth in the CSP sector. Conversely, policies for CFP generation in China are more stringent, focusing on reducing coal dependence, improving energy efficiency, and promoting low-carbon practices. This includes strict regulation of new projects to decrease coal electricity’s share, enforcing international standards for lower emissions, and driving operational flexibility reforms to adapt to future market dynamics. Collectively, these efforts aim to transition to a more sustainable and adaptable power generation paradigm, demonstrating China’s commitment to sustainable advancement and energy system transition.

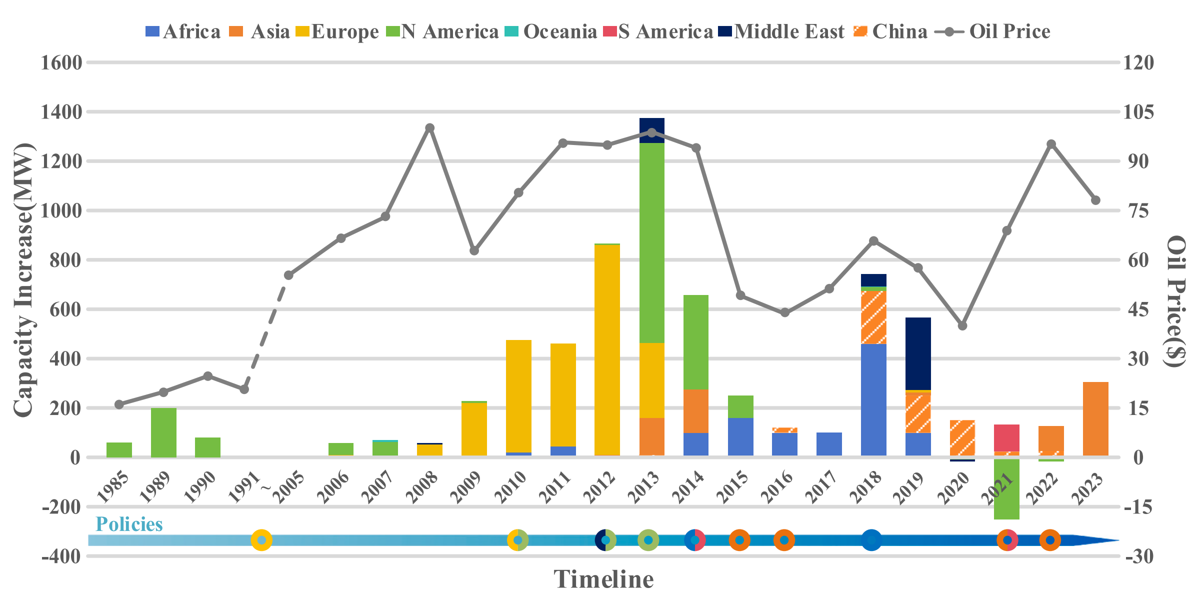

Fig. 3. . The historical development curve of newly installed CSP capacity and oil prices [46–49], [61], [62], [71–79].

2.2. Technical characteristics and development status

2.2.1. Technical development history

The symbiotic evolution of theoretical foundations and engineering applications constitutes a pivotal trajectory for the advancement of the CSP sector. Beginning in the early 20th century, researchers embarked on pioneering theoretical explorations and engineering demonstrations in CSP. Notably, Professor Giovanni Francia designed and built the first CSP experimental station with a structure similar to modern plants, which began operation in Sant'Ilario, Italy, as early as 1968 [57]. However, as shown in Fig. 3 and Fig. 4, it was not until the 1980s that CSP technology experienced significant advancements, epitomized by the construction of the SEGS I in California in 1984 [58], the world's first commercial CSPP. This pivotal development was followed by the establishment of SEGS II to VII between 1984 and 1991, demonstrating the viability of trough-type CSP generation on a larger scale. Early CSP installations predominantly utilized thermal oil as the heat transfer fluid, a choice that limited thermal efficiency to about 36 % due to the temperature constraints (up to 390 °C) of the thermal cycle system [8]. Additionally, to address the inherent variability and unpredictability of solar irradiance, these facilities were equipped with supplementary gas turbines to ensure stable and controllable power output, consequently leading to high construction and operational costs. Therefore, as depicted in Fig. 3, the subsequent downturn in oil prices in the 1990s led to a rapid contraction of CSP incentive policies, resulting in a prolonged developmental hiatus. Despite this setback, the period of stagnation was marked by persistent research efforts aimed at identifying and rectifying the technological limitations of early CSP systems. Among the various solutions explored, TES technology emerged as a significant breakthrough, showcasing superior performance in pilot implementations [59], [60]. Between 2007 and 2013, under the stimulus of Spain's refined feed-in tariff regulations [61], [62], TES technology was extensively integrated into 50 newly established CSP projects across Spain. In this period, driven by a combination of technological advancements and escalating oil prices, a series of CSP stations, represented by the Nevada Solar One plant and Crescent Dunes plant, were sequentially commissioned in the United States [63], [64], collectively achieving a capacity nearing 1000 MW. The integration of TES in these installations transformed CSP into a dispatchable and stable source of clean energy.

Concurrently, there was a concerted push within both academic and industrial circles towards the adoption of novel heat transfer mediums. As described in Fig. 4, a notable example is the Archimede plant in Italy, built in 2010, which pioneered the use of molten salt as both a heat transfer and storage medium, thereby substantially enhancing the thermal efficiency of CSP systems [65]. This achievement marked the inaugural application of second-generation CSP technology in a practical engineering setting, heralding a new phase in the sector's evolution. Following this, countries with abundant solar resources like Morocco [66], [67], South Africa [68], [69], and the United Arab Emirates [70] also embarked on the exploration and construction of CSPPs, with most projects integrating long-term molten salt TES systems.

Since 2016, driven by the dual-carbon goals, China's CSP industry has undergone rapid development and expansion. By 2023, the installed capacity of CSP in China had reached approximately 588 MW. Additionally, over 4 GW of CSP projects were either in the planning stages or under construction, with grid connections expected to be completed by 2025 [39]. Currently, China's second-generation CSP technology has reached a stage of maturity, characterized by the widespread adoption of molten salt as the heat transfer fluid alongside the implementation of ultra-long TES systems, capable of storing energy for up to 13 h. Furthermore, China is actively pursuing research and development efforts towards the next generation of CSP technology. This includes the successful development of supercritical carbon dioxide power generation prototypes and the commencement of construction on the first 10 MW supercritical carbon dioxide Brayton cycle demonstration power plant [8].

As depicted in Fig. 4, CFP generation, when compared to CSP, has consistently held a dominant position in terms of cycle efficiency. As

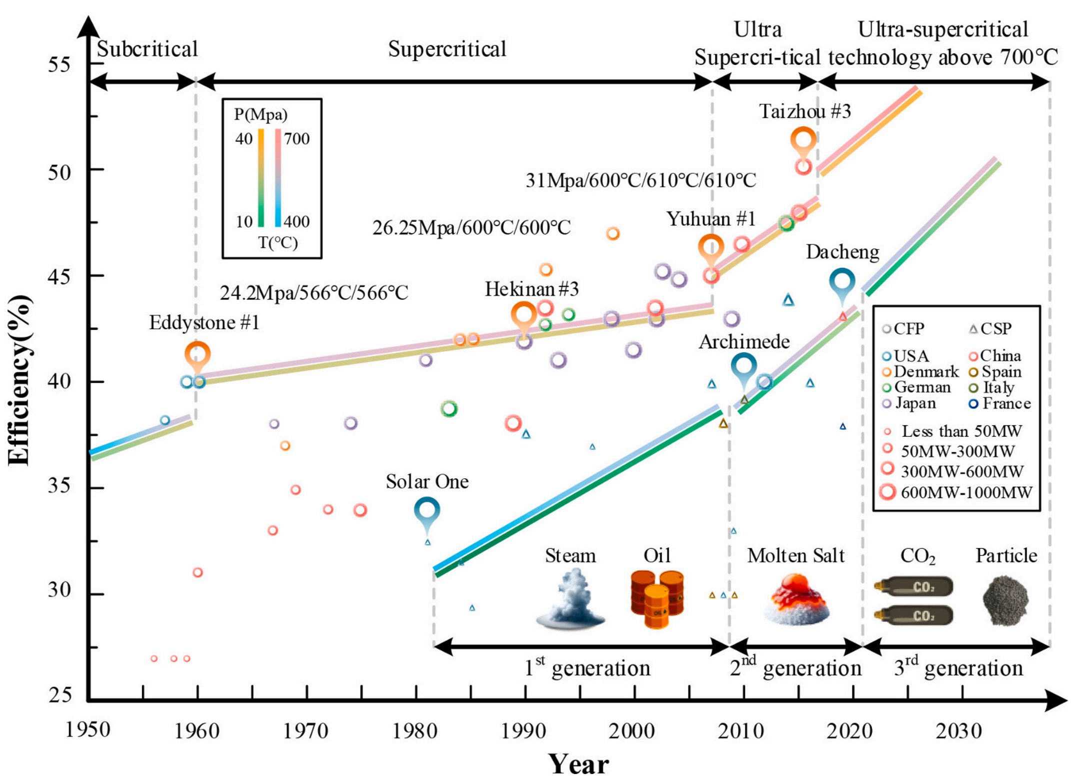

Fig. 4. . Schematic diagram of the technological evolution of CFPPs and CSPPs [8], [39], [65–70], [80–85].

early as the late 1950s, the United States took the lead in researching and applying supercritical power generation [80]. In 1957, the first supercritical power generation plant was declared to be in commercial operation, marking a significant advancement in thermal power generation technology. Subsequently, new power plants in the United States adopted higher steam parameters (24.1 MPa/566 °C) after 1960, contributing to the gradual maturation of supercritical power generation technology [81]. In the 1970s, Japan also successfully mastered supercritical power generation technology through a route of introduction, imitation, and innovation [82]. Furthermore, countries like Germany, Denmark, and the former Soviet Union were among the pioneers in developing and mastering supercritical power generation technology [80], [83]. Comparatively, China's CFP technology started later, with the introduction of subcritical power generation technology in the early 1980s [84]. After more than two decades of technological research and development, China achieved significant progress with the operation of the domestically produced ultra-supercritical unit, Yuhuan Power Plant Unit 1, in 2006. Subsequently, China's ultra-supercritical once-through reheating unit, Guodian Taizhou Power Plant Unit 3, built in 2015, reached the international leading level in terms of efficiency [85].

Overall, from the perspective of cycle efficiency, there remains a considerable gap between CSP and CFP generations. Supercritical power generation technology is fully mature in CFP generation, while CSP predominantly uses subcritical power generation technology. Future research should focus on exploring new heat transfer fluids and adopting new cycle power generation modes to achieve higher cycle temperatures and pressures, thereby enhancing CSP generation efficiency and reducing costs.

2.2.2. Structural characteristics

2.2.2.1. Structure principal. As shown in Fig. 5, the CSPP can be mainly divided into three subsystems: solar field, TES system, and power block. Take linear Fresnel CSPP as an example, with the control of the tracking system, the solar energy is firstly reflected by the flat mirrors and then focused by a second compound parabolic concentrator. The concentrated solar energy is absorbed by a central vacuum receiver to heat the inside molten salt. At the rated condition, the inlet cold molten salt (290–300 °C) is heated by the collected solar energy to approximately 550 °C. The TES system consists of a cold tank and a hot tank and can provide a long-term stable supply without sunlight. As for the power block, it can be further divided into SGS, steam turbine, electrical generator, feedwater heat exchanger, and condenser. The steam generation system includes preheater, evaporator, steam drum, superheater, and reheater. As shown in Fig. 5, the preheated feedwater is pumped into heat exchanger trains and heated into superheated steam. The high-pressure superheated steam then spins the turbine to turn thermal energy into mechanical energy. Finally, the electrical generator is pulled by the steam turbine to produce active and reactive power with proper excitations [86–89].

By comparing Fig. 5 and Fig. 6, subcritical CFPPs and CSPPs exhibit certain structural similarities; however, they differ significantly in their energy supply modes, leading to distinct structural and operational characteristics. 1) *Front-end energy supply system*: Unlike the "solar-heat-electricity" transfer process in CSPPs. The subcritical CFPP burns coal in the boiler to release the chemical energy and generates high-temperature and high-pressure steam for power generation. Compared to the solar field system, the combustion system in CFPPs is more intricate and extensive, comprising coal handling, boiler combustion, air and flue gas, and ash handling systems. The large and complex front-end energy supply system of CFPPs results in slower output regulation compared to CSPPs. 2) *Steam generation system*: Differences in the physical properties of the high-temperature heat transfer fluids determine the differences in the structure and control design of steam generation systems between CSPPs and CFPPs. CSPPs employ shell-and-tube heat exchangers, whereas CFPPs utilize convection-radiation heat exchangers. This structural disparity influences the design of control systems, such as steam temperature regulation methods (water spraying control in CSPPs vs. cold salt control in CSPPs) [90], [91]. 3) *Power generation system*: Both power plants employ steam turbines to generate electricity; however, there are notable disparities in the performance requirements of the turbines. As presented in Table 1, turbines in CSPPs must fulfil design specifications for frequent and rapid start-stop operations, necessitating lower rotor mass [92], [93]. Furthermore, to enable continuous low-load operation during nighttime and adaptability to frequent variable operating conditions, CSP turbines have higher material requirements in their design.

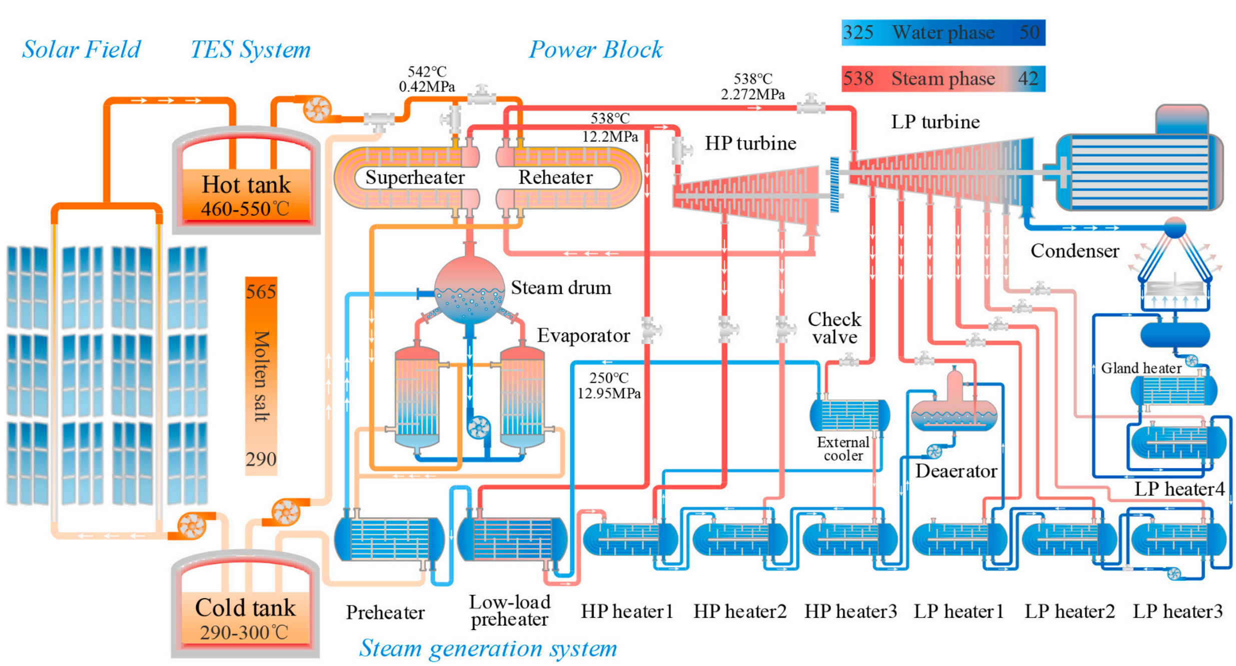

Fig. 5. Schematic diagram of the linear Fresnel CSPP with direct molten salt storage [90].

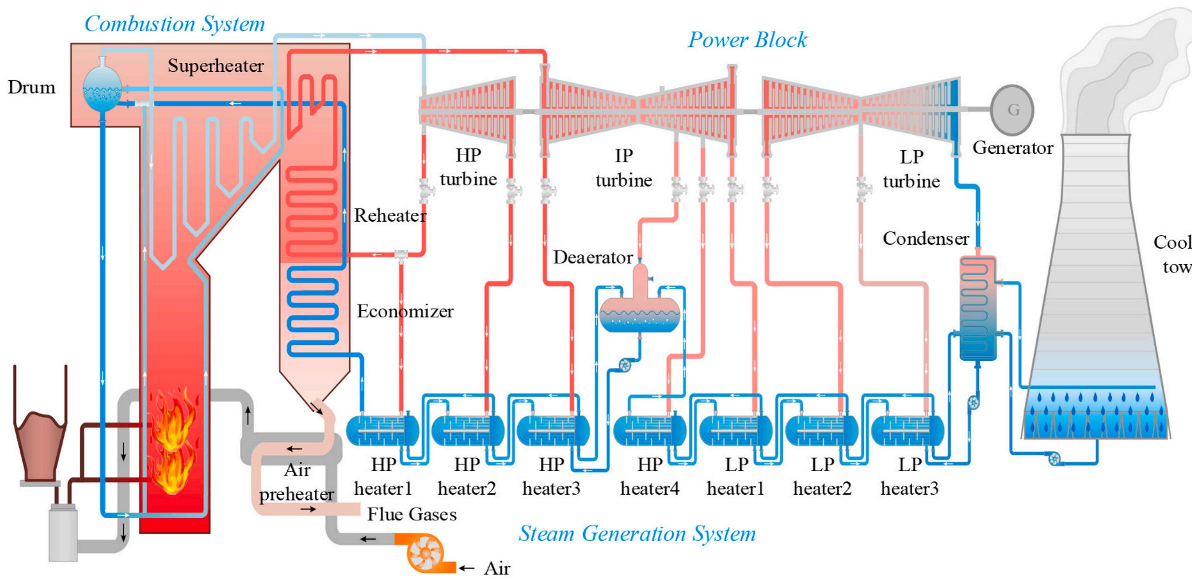

Fig. 6. Schematic diagram of the subcritical CFPP.

Table 1
Differences between steam turbines of CSP and CFP.

Requirements	CSP	CFP
Daily start and stop	Required	Not required
Hot startup time	Less than 25mins	60 min
Cold startup time	60 min	240 min
Ramp rate	5 %/min	1.5–2 %/min
Output	Base load and peak load	Base load
Load range	15–100 %	50 %–100 %
Temperature variation rate	10 °C/min	1.5–5 °C/min
Rotor volume	Smaller	Bigger

2.2.2.2. Control system. The control system of CSP can be mainly divided into two parts: the front-end solar collecting and thermal storage control system, and the back-end power block control system. Since the front-end control systems of CSP and CFP address different energy conversion processes, the CSP front-end solar concentration control system and the CFP front-end combustion control system are vastly different and not comparable. In contrast, the back-end structures of both systems are relatively similar, providing some comparability in their control system architectures. As shown in Fig. 7, the control system of a CSPP inherits the two-level control structure from a traditional CFPP [94–96]. The primary control level can be mainly divided into two parts according to their functions. The first part receives external and manual signals and converts them into reasonable setting values of load and pressure demand. In the second part, the demand master signals are produced through a series of signal processing and control blocks. The produced signals are then distributed to various control subsystems at the secondary level to fulfil the required tasks.

According to Fig. 7, the power control strategy of a CSPP is broadly similar to the one of a CFPP. However, there still exist some differences due to its special energy-supplied mode and component structures [89–91]. According to our previous studies [90], [91], hot salt flow control and steam temperature control show distinctive differences compared with the ones in a CFPP. Taking steam temperature control as an example, the cold salt adjustment method but not the traditional water spraying method is adopted in a CSPP to control the steam temperature. As shown in Fig. 8, the steam temperature control can be divided into two parts. The first part adjusts the cold salt with the corresponding salt pump. The second part deals with the distribution of hot salt to keep a balance between the temperatures of superheated steam and reheated steam. The main reasoning is that the indivisible U-shape tube-and-shell superheater and reheater are adopted in a CSPP, unlike the traditional ones with multiple sections. In this situation, the regulation efficiency of the traditional method is greatly reduced. More importantly, the theoretical analysis and practical experiences show that the temperature control speed with cold salt in a CSPP is usually faster than the one in a CFPP. This means the former can undertake larger and quicker load variations [97].

3. Potential comparison of CSP versus CFP

3.1. Methodology for assessing CSP and CFP potentials

To assess the viability of CSP as a substitute for CFP, this study conducts a comprehensive comparative analysis from three perspectives: geographical, technical, and economic, corresponding to the three parts presented in Fig. 9. The first perspective focuses on the geographical potential of CSP and CFP. Using the AHP and GIS data, the study evaluates and compares the land suitability of different regions for implementing CSPP as a replacement for CFPP. Based on the geographical assessment, the study proceeds to calculate the technical installed capacity and generation capacity of CSP within the identified feasible regions. This estimation is carried out using a CSP technical potential evaluation model. By comparing the potential of CSP with the existing installed capacity and electricity generation of CFP in each region, the technical feasibility of CSP replacement solutions in different regions can be determined. Finally, the economic feasibility of replacement solutions is examined by spatially calculating the LCOE in each region. This analysis provides insights into the cost-effectiveness of CSP compared to CFP in different regions. It is important to note that this section extensively utilizes GIS data, which is further detailed in Section A1 of the supplementary material.

3.1.1. Assessing geographical potential

The geographical potential of solar generation in a selected area refers to the amount of total yearly solar radiation available in that area, considering existing geographical constraints such as forests and waterbodies [98–101]. According to Fig. 9, the process of geographic potential analysis involves the elimination of restrictive areas followed by a weighted analysis of the selected evaluation criteria to determine the geographic potential classification. The specific details of the geographical potential analysis process are described below.

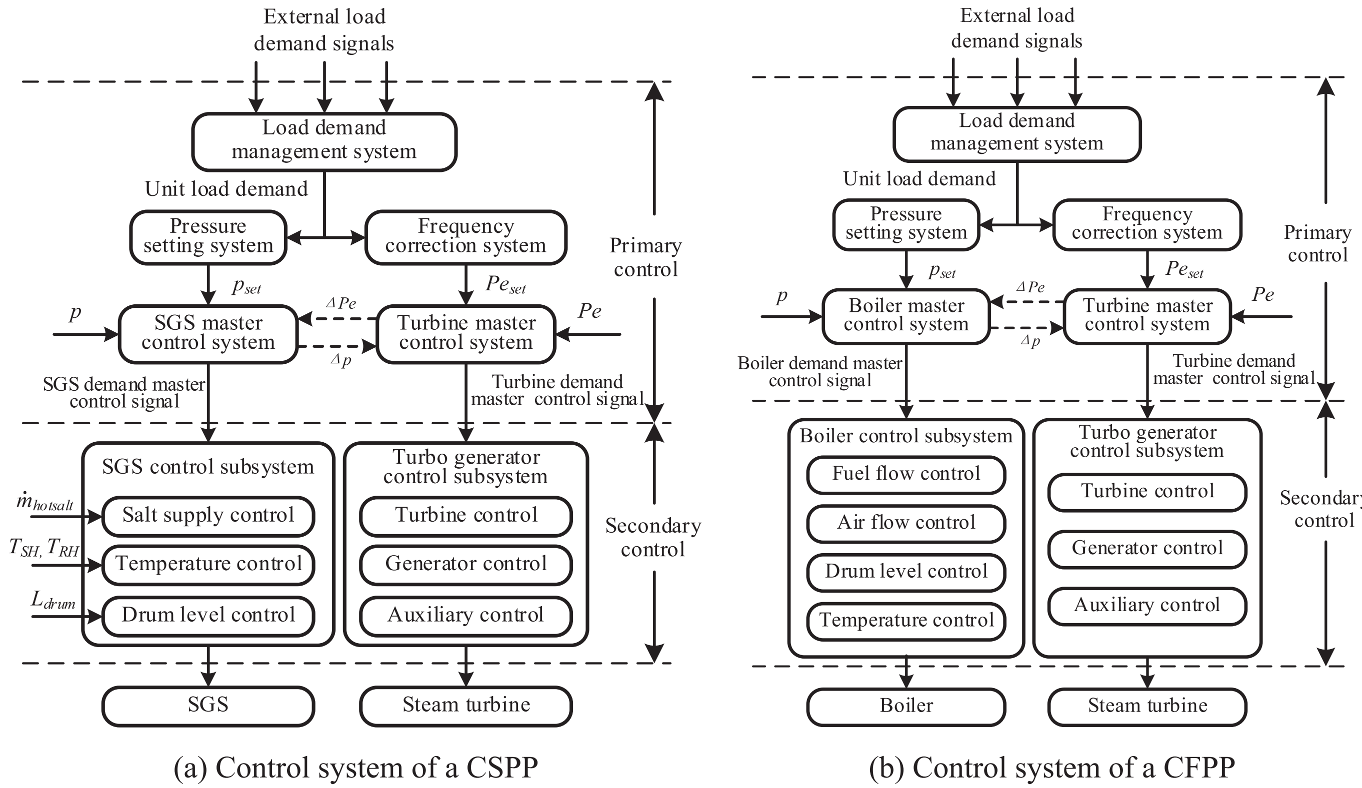

Fig. 7. Hierarchical control systems for CSPPs and CFPPs [91].

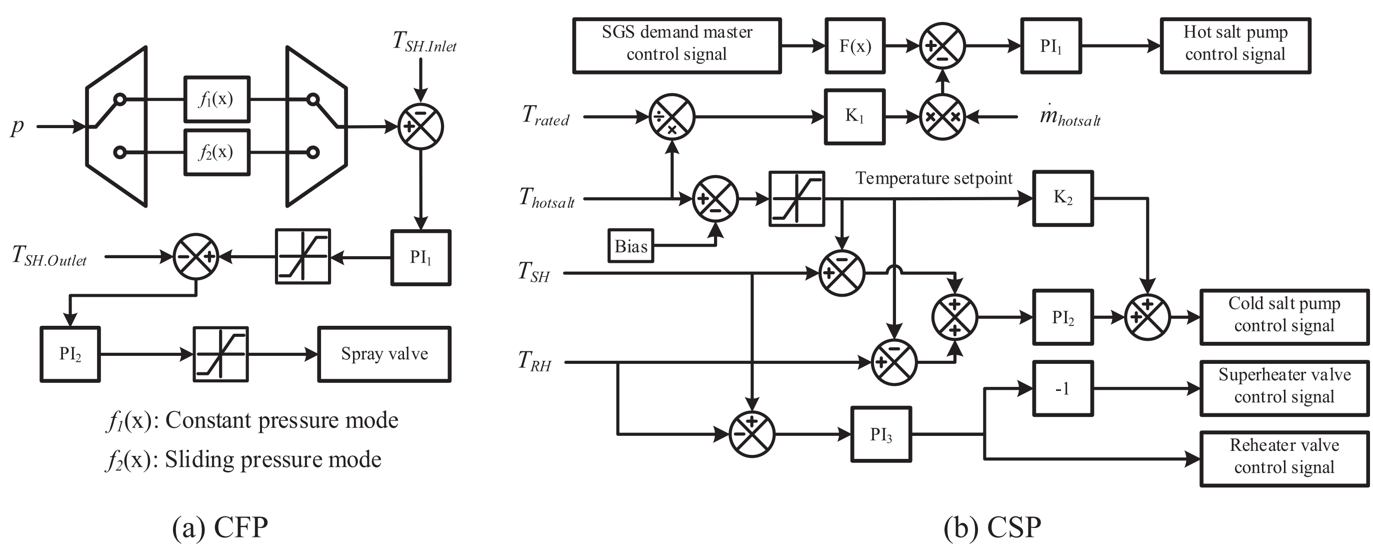

Fig. 8. Comparison of steam temperature control systems in CSP and CFP [91].

3.1.1.1. Exclude restrictive areas. As shown in Table 2, two types of criteria are usually considered to exclude restrictive areas, i.e., mandatory restrictive criteria and quantitative restrictive criteria [101]–[104], [111], [112]. The latter is typically straightforward to measure, such as DNI, and the area will only be excluded if the chosen criteria exceed a specific threshold value. This paper selects a series of restrictive criteria with the highest degree of recognition based on the literature review results presented in Table 2, including protected areas, land cover, slope, DNI, etc. It is important to note that the minimum limit of DNI of 1800 kWh/m^2, which is commonly used in most literature, may not be directly applicable to China's unique geographical conditions. This is because China's areas with abundant solar energy resources are mainly located in high latitudes, and the solar energy resources in these regions are not as abundant as those in equatorial regions. To better fit China's actual national conditions and in line with the regulations of China's NEA, this paper relaxes the minimum limit of DNI to 1600 kWh/m^2 [98].

3.1.1.2. AHP method. After eliminating restrictive areas, the next step is to identify appropriate evaluation criteria for assessing the suitability of the remaining areas. To ensure the considered criteria are recognized by both the research community and industry, a comprehensive literature review and industrial investigation are carried out [100–118]. For CSPPs, a review of relevant literature summarized in Fig. 10 reveals that climate, orography, location, economic, and environmental aspects are

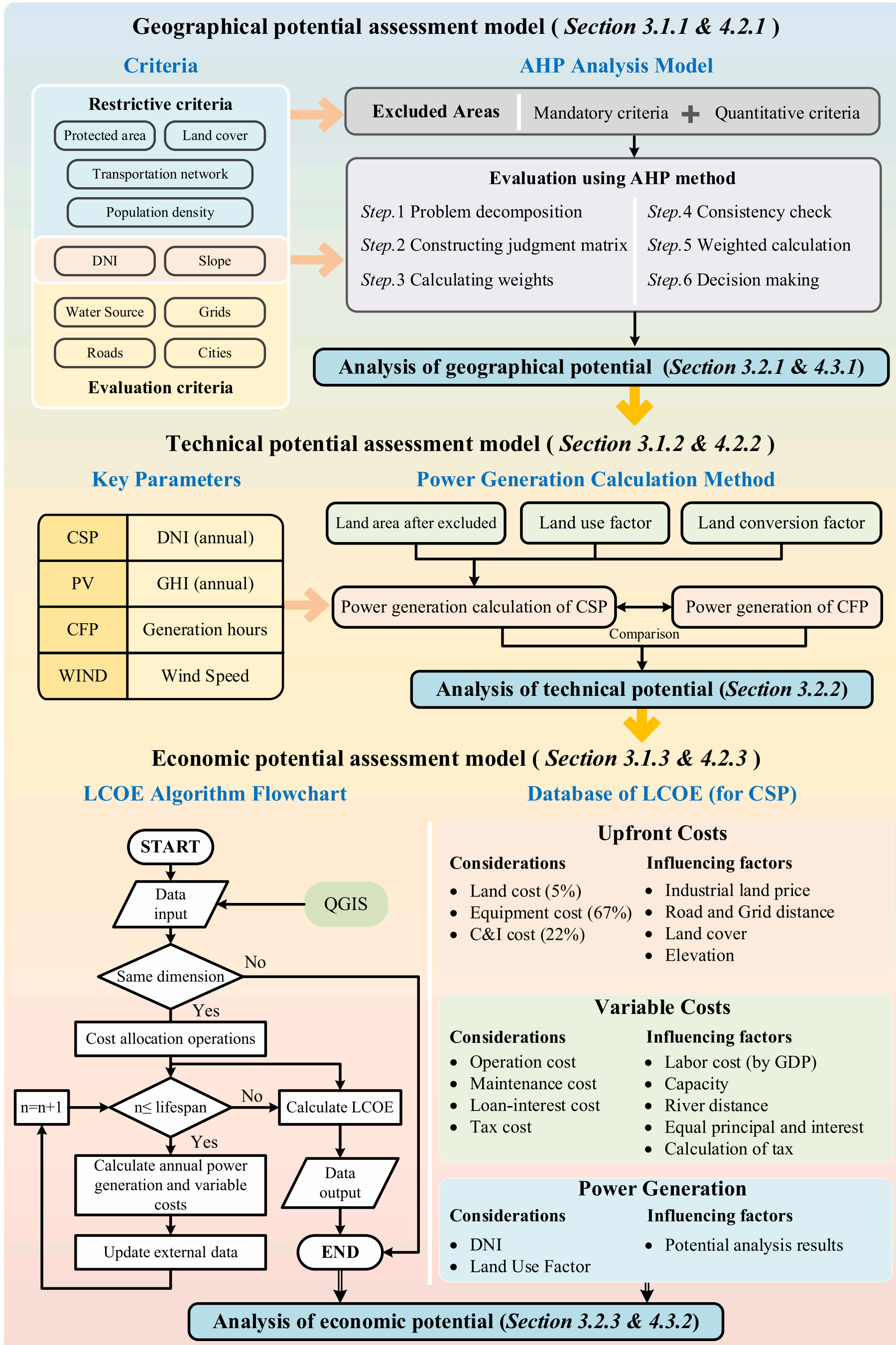

Fig. 9. . Flowchart of the potential comparison process.

the primary evaluation criteria to be considered in making informed decisions. In the case of CFPPs, this paper combines existing research and relevant construction regulations to determine the evaluation criteria [119], [120]. Finally, the selected criteria are summarized in Table 3.

As depicted in Table 3, the evaluation criteria utilized in this study are classified into five classes to represent the different suitability. To determine the relative importance of these criteria, the widely used AHP is employed in this paper. AHP involves several key steps, including the construction of a hierarchical structure, pairwise comparisons, and calculation of weights. Among them, the pair-wise comparison process is a particularly crucial part. In our study, such comparisons are conducted by utilizing statistical data in Fig. 10 and consulting with specialists in the field. The outcomes of these comparisons are then used to derive the overall weights assigned to each criterion. As illustrated in Fig. 10, the obtained weights for CSP demonstrate a high level of consistency with the statistical results obtained from the literature review, which implies the obtained weightings are reasonable. For a more comprehensive understanding of the calculation and analysis of AHP methodology, additional details are provided in Sections A2 and A3 of the supplementary material.

3.1.2. *Assessing technical potential*

Based on the geographical potential analysis, suitable regions for deploying CSPPs are identified. According to Fig. 9, a technical potential analysis is conducted to calculate the theoretical technical generation capacity and installed capacity of CSP within the selected regions. The obtained results are then compared with the practical power generation

Table 2
Restrictive criteria for CSP and CFP.

Criteria Type	Criteria	Description	Buffer	Literature
Mandatory	Protected area	World heritage sites, national parks, and IUCN class I-VI	0.5 km	[100][101][102][103][104]
	Urban settlements	Urban settlements with over 10,000 inhabitants	1 km	[102][104][105][106]
	Land cover	Wetlands, forests, grasslands, water bodies, and agricultural lands	0.25 km	[100][101][107][108][109]
	Transportation network	Railways and roads	0.25 km	[103][104][105][110]
Quantitative	DNI	1600 (kWh/m^2/year) for CSP	No	[101][102][104][111][112]
	Slope	>3° for CSP[98] and > 8° for CFP[99]	No	[101][104][108][111][113]
	Population density	>500 inhabitants/km^2	No	[102][112][114][115]

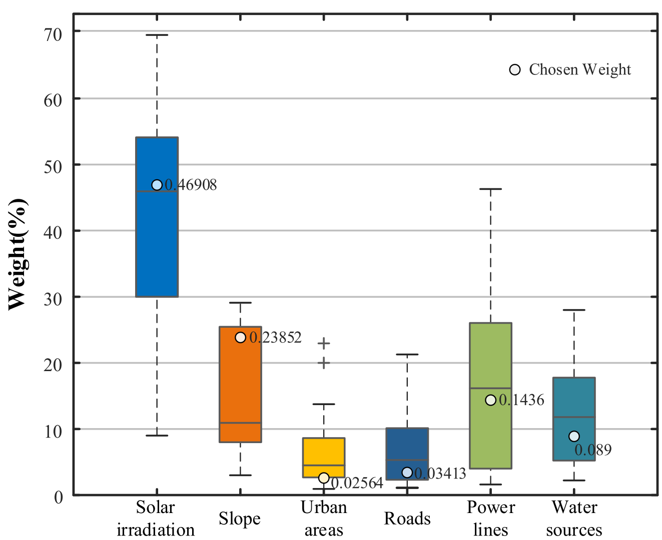

Fig. 10. . Summary of criteria and weights used in the relevant literature [100–105], [109–112], [121–134].

and installed capacity of CFPPs to assess the feasibility of substituting CFP with CSP in different provinces. In this study, eqs. (1) and (2) are utilized to calculate the technical generation capacity and installed capacity, respectively [106], [108], [135]. However, it should be noted that the statistical data available for the coefficients in these equations may not apply to the specific context of China. To address this limitation, an extensive and comprehensive review of practical CSPPs in China is conducted, and the coefficient values used in this study are based on the findings of this review. Further details regarding the comprehensive information review process can be found in Section A4 of the supplementary material.

Table 4 highlights the variations in the land-use efficiency (LUE) and land conversion factor (LCF) among different types of CSP generation technologies [108], [135], [136]. These variations primarily stem from the differences in solar field configurations. Besides, the solar-to-electric conversion efficiency is influenced by many factors, including solar concentration, heat transfer fluid, power cycle efficiency, etc. In this paper, to account for these factors and their impact on the technical potential, both upper and lower limits are considered when calculating the ranges of the technical potential values.

$$Cap_{generation} = LA^{*}LUE^{*}DNI^{*}\eta \tag{1}$$

$$Cap_{installed} = LA^{*}LCF \tag{2}$$

3.1.3. Assessing economic potential

To evaluate and compare the economic potential of CSP and CFP in China, the LCOE is calculated for different regions using the discounting method, which considers the cost and depreciation of the entire project life cycle (as shown in (3)) [19], [137]. To obtain the spatial distribution of LCOE for CSP and CFP, various spatial factors such as geographical conditions, policy incentives, and economic conditions that may influence LCOE calculations in different regions are considered. As depicted in Fig. 9, the overall process for LCOE calculation includes data input, coefficient adjustments, and LCOE computation. To calculate the adjustment coefficients ($k_{land.i}$, $k_{system.i}$, $k_{CI.i}$, $k_{OM.i}$, $k_{F.i}$) for cost items, this study compares the input data for each raster point with the benchmark data from a reference power station. Then, Eq. (6), combined with Eq. (3)–(5), is utilized to compute the LCOE for that specific raster point ($LCOE_i$). As for the benchmark power station, this study selects a 100 MW tower-type CSPP located in Dunhuang, Gansu, as the reference. This plant is equipped with an 11-h TES system, occupies an area of 8 km^2, has a total static investment of 3 billion yuan, and an assumed life span (N) of 25 years. For more detailed information about the benchmark power stations, please refer to Section A7 of the supplementary material.

Table 4
Technical parameters of three different CSP generation technologies.

Technology	LUE (%)	LCF (MW/km^2)	η (%)
Parabolic trough	25	20	11–21
Power tower	16	13	15–35
Linear Fresnel	40	16	8–18

Table 3
Criteria and weights of geographical potential evaluation for CSPPs and CFPPs.

Criteria for CSPP	*Classes*						*Criteria for CFPP*	*Classes*					
	L5	L4	L3	L2	L1	W (%)		L5	L4	L3	L2	L1	W (%)
DNI (kwh/m^2/year)	>2300	2100–2300	1900–2100	1700–1900	1600–1700	44.881	Distance to collieries (km)	0–5	5–15	15–30	30–50	>50	37.262
Slope (°)	0–0.5	0.5–1	1–2	2–2.5	2.5–3	25.461	Slope (°)	0–2	2–4	4–6	6–8	>8	14.482
Distance to grids (km)	<5	5–10	10–15	15–20	>20	14.700	Distance to grids (km)	<5	5–10	10–15	15–20	>20	10.348
Distance to water (km)	<10	10–20	20–30	30–40	>40	8.367	Distance to water (km)	<10	10–20	20–30	30–40	>40	24.07
Distance to roads (km)	<10	10–15	15–20	20–25	>25	4.075	Distance to roads (km)	<10	10–15	15–20	20–25	>25	10.669
Distance to urban (km)	5–10	10–20	20–30	30–40	>40 / <5	2.517	Distance to urban (km)	5–10	10–20	20–30	30–40	>40 / <5	3.169

Note: L5: Best suitable; L4: Highly suitable; L3: Moderately suitable; L2: Marginally suitable; L1: Less suitable; W: Weight.

The specific details of the LCOE calculation are described as follows:

$$LCOE_{ref} = \frac{C_{initial.ref} + \sum_{n=0}^{N} \left(C_{annual\_n.ref}(1+r)^{-n}\right)}{\sum_{n=0}^{N}\left(E_n(1+r)^{-n}\right)} \tag{3}$$

$$C_{initial} = C_{land} + C_{system} + C_{CI} + C_{other} \tag{4}$$

$$C_{annual\_n} = OM_n + I_n + L_n + T_n + F_n \tag{5}$$

$$LCOE_i = \frac{C_{land}k_{land.i} + C_{system}k_{system.i} + C_{CI}k_{CI.i} + \sum_{n=0}^{N}\left((OM_n k_{OM.i} + I_n + L_n + T_n + F_n k_{F.i})(1+r)^{-n}\right)}{\sum_{n=0}^{N}\left(E_{n.i}{}^{*}(1+r)^{-n}\right)} \tag{6}$$

3.1.3.1. Initial costs. According to Eq. (3), the lifecycle cost comprises both the initial cost ($C_{initial}$) and the annual cost (C_{annual_n}). The initial cost can be further categorized into land costs (C_{land}), system costs (C_{system}), construction, and installation costs (C_{CI}). Notably, there are significant differences in land costs among different provinces due to their varying land policies. In China, land use rights for industrial projects can be acquired through allocation, grant, or transfer. For CSP projects, the land use rights for the first batch of demonstration projects were initially allocated to the CSP companies by the local government at a minimal cost. However, with the increasing experience in project development, subsequent CSP projects have required obtaining land through grants, which typically accounts for 5 % of the total static investment. For CFP projects, the portion of land cost is higher, typically 10 %, since CFP projects are more concentrated in the east areas with higher land prices. To consider the impact of regional variations in land prices, as shown in Fig. A3, this study employs the Industrial Land Price Coefficient ($k_{land.i}$), defined as the ratio of local land prices (LP_i) to reference industrial land prices (LP_{ref}) in Eq. (7), to calculate land costs in each province. The construction and installation costs (C_{CI}) are influenced by various factors, and this study employs the AHP method to comprehensively consider the effects of temperature, altitude, distance to roads, and distance to the power grid. In the final LCOE calculation, adjustments to the construction and installation costs are made with a 5 % increment for each level difference. Regarding the system costs, since equipment prices are relatively consistent across the country, a fixed ratio is used for calculation purposes.

$$k_{land.i} = \frac{LP_i}{LP_{ref}} \tag{7}$$

3.1.3.2. Annual costs and electricity generation. As the second main part of the lifecycle cost, the annual costs encompass various elements such as operation and maintenance cost (OM_n), insurance fees (I_n), loan interest cost (L_n), tax cost (T_n), and fuel cost (F_n) applicable only to CFP. The O&M cost mainly comprises labour expenses and equipment maintenance costs. For labour expenses, the latest per capita gross domestic product (GDP) data for each prefecture-level city in 2023, as shown in Fig. A2, is utilized for calculation. As for equipment maintenance costs, they are influenced by local economic conditions, proximity to water sources, frequency of rainfall, sandstorm occurrence, and other factors. To consider these factors comprehensively, the AHP is employed. Regarding insurance fees (I_n), they are generally not affected by spatial factors and typically account for 0.5 % of the total static investment. The loan interest costs (L_n) are calculated using the equal principal and interest method, considering the latest interest rate of 4.2 % in 2023. For tax costs, CSP projects usually benefit from a 50 % reduction in taxes, whereas CFP projects are subject to additional environmental taxes. Furthermore, CFP requires special consideration of the fuel cost, which includes both the purchase and transportation fees of the power coal. The former is calculated based on the ratio between coal consumption and electricity generation, while the latter employs the latest transportation data. As for the discount rate (r), a typical value of 10 % is adopted in this paper [138], [139].

For the calculation of annual electricity generation (E_n), this study directly employs the power generation potential model from section 3.1.2 to determine the annual electricity generation of equivalent 100 MW CSP power plants in each raster. As for the annual electricity generation of CFP, it is calculated by multiplying the capacity by the actual average power generation hours for each province from 2022 to 2023, as shown in Fig. A5 [4]. For more key parameters and LCOE calculation details, please refer to Section A5 of the supplementary material.

3.2. Analysis of CSP and CFP potential results

3.2.1. Analysis of geographical potential results

According to the evaluation criteria presented in Table 3, individual suitability maps for each criterion can be generated, as depicted in Fig. 11. From the perspective of natural resources, regions with abundant DNI resources are predominantly found in northwest areas such as Tibet, Inner Mongolia, Qinghai, Xinjiang, and Gansu. Conversely, coal mining resources are concentrated in regions like Shanxi, Inner Mongolia, Shaanxi, Xinjiang, and Guizhou. As for the distribution of road networks, power grids, water resources, and dense population centres, they exhibit an “east dense, west sparse” pattern. For detailed information on the divisions of Chinese provinces and regions, please refer to Section A6 of the supplementary material.

Based on the criteria in Table 2, the restrictive area is obtained and eliminated. Subsequently, by overlaying and weighting the individual suitability maps, the final land suitability maps for CSP and CFP generations in China can be derived as Fig. 12. The statistical results in Fig. 13 reveal that approximately 78.4 % of the regions are deemed unsuitable for CSP, primarily due to two key factors: 1) China’s high latitude results in many regions not meeting the minimum DNI requirements for CSP. 2) the need for high slope angles poses a significant limitation on CSP development. Despite these restrictions, a substantial area, approximately 2.06 million km^2, remains available for CSPP construction, predominantly in the northwest regions such as Qinghai, Gansu, Xinjiang, Tibet, and Inner Mongolia.

In the case of CFP, the suitable land area for construction has been estimated at 5.07 million km^2, which is around twice the area available for CSP. The most favourable regions for both technologies are primarily located in Xinjiang and Inner Mongolia, positioning these provinces as prime locations for CSP pilot or demonstration projects as sustainable alternatives to CFP. Furthermore, regions in Central and Eastern China, such as Shandong, Shanxi, and Henan, with their rich coal mine resources, also possess valuable land resources for constructing CFPPs. A review of Fig. 12 and Fig. 13 reveals that the geographical distributions of suitable regions for CSP and CFP show complementary characteristics, reducing direct competition and facilitating the strategic development of CSP in regions where it has distinct advantages.

To demonstrate the effectiveness of this evaluation method, the study compares the distribution of existing power plants with the land suitability map. As indicated in Table 5, more than 90 % of CFPPs are situated in level 5 and level 4 regions, and 86 % of CSPPs are located in level 3, level 4, and level 5 regions. However, there are still six power plant projects (14 %) located in level 2 regions, primarily due to the

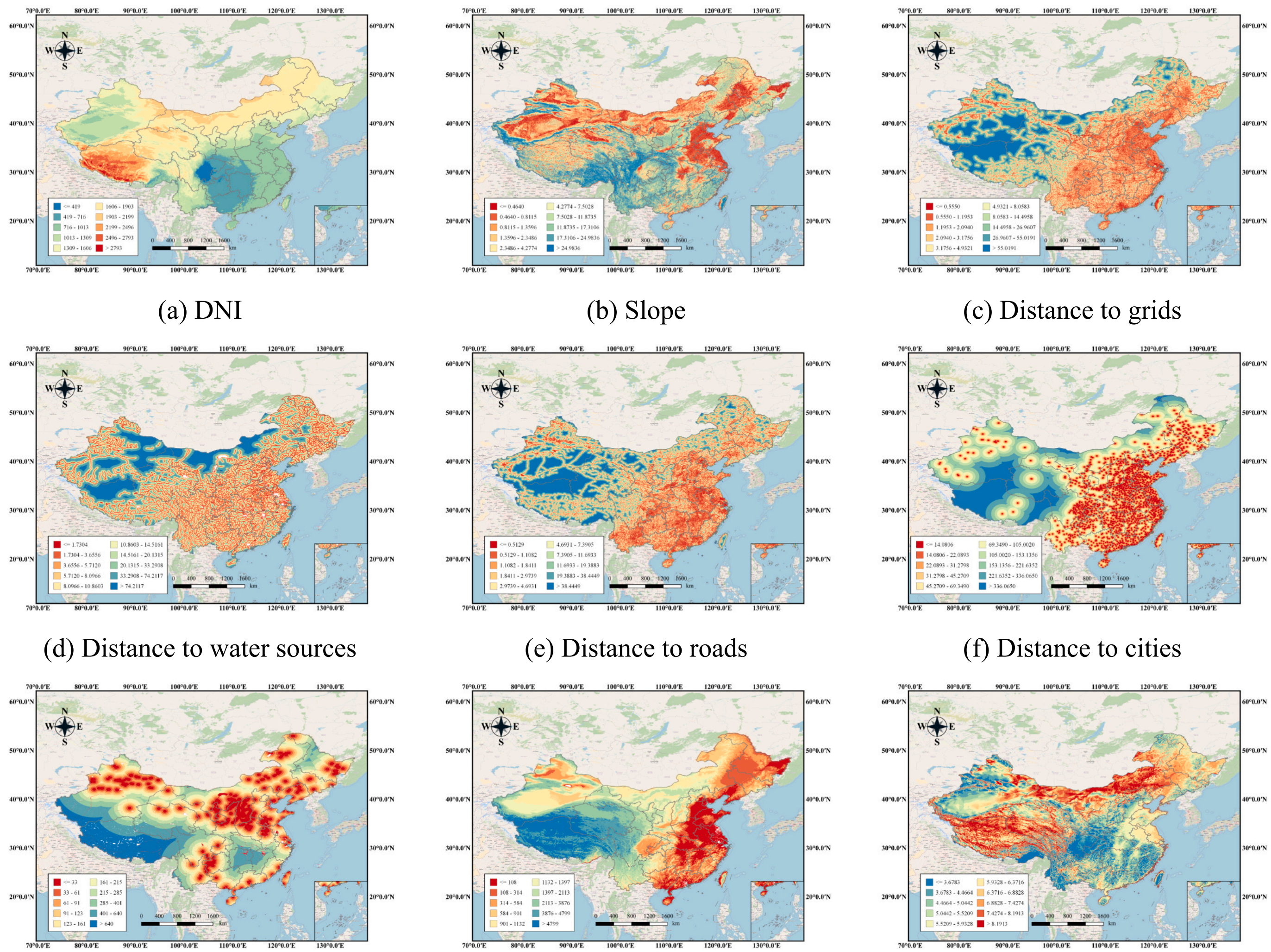

(a) DNI (b) Slope (c) Distance to grids

(d) Distance to water sources (e) Distance to roads (f) Distance to cities

(g) Distance to mines (h) Elevation (i) Wind speed (100m)

Fig. 11. Suitability classification maps of evaluation criteria.

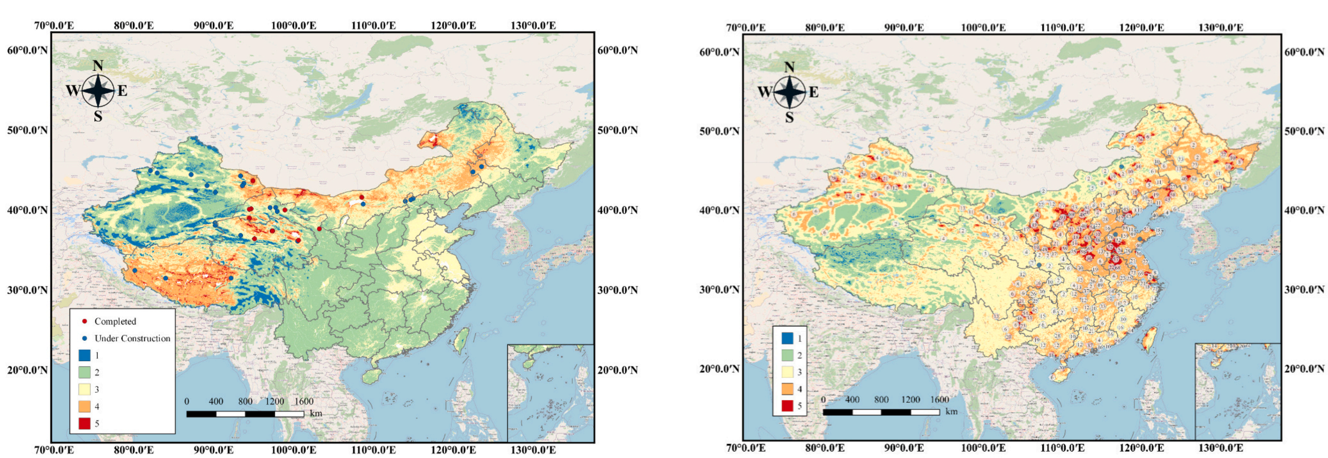

(a) CSP (b) CFP

Fig. 12. Land suitability maps for CSP and CFP

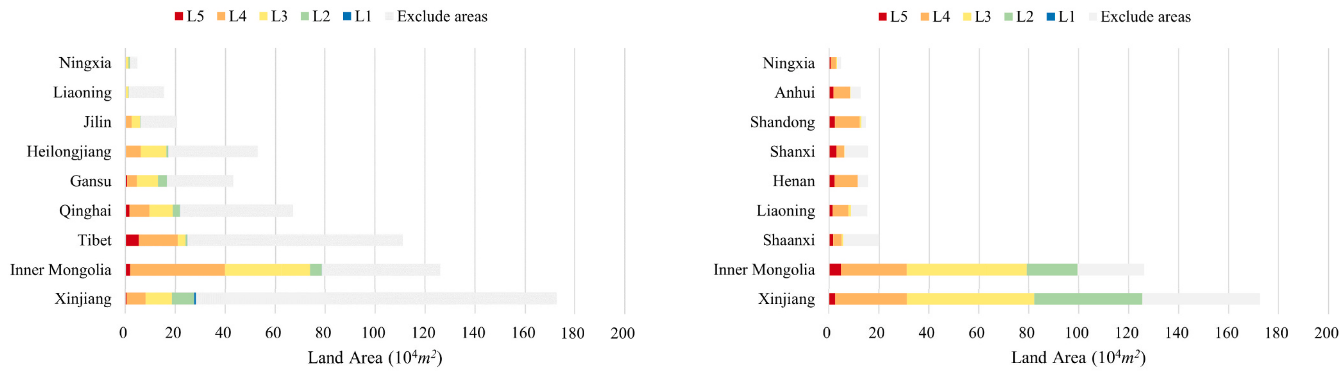

(a) CSP (b) CFP

Fig. 13. Distribution of different levels of areas in each province.

Table 5
Verification results of land suitability maps.

	Level	L5	L4	L3	L2	L1
CSP	Number	3	20	13	6	0
	Percentage	7.14 %	47.62 %	30.95 %	14.29 %	0.00 %
CFP	Number	2035	2863	321	4	0
	Percentage	38.96 %	54.82 %	6.15 %	0.08 %	0.00 %

following two reasons: 1) CSP power plant construction is still relatively limited, with most projects being demonstration projects driven by national or regional policy subsidies, which allows more flexibility in site selection. 2) In some regions, there is a notable discrepancy between ground-based measurements and satellite measurements of DNI, leading to rating deviations. Particularly in the Xinjiang region, the lack of Solargis ground stations leads to discrepancies between model predictions and actual measurements, with variances up to ±12 %. Real-world comparisons show that Solargis data tends to underestimate actual observations by about 200 kWh/m^2/year in this area. Therefore, this study's assessment of Xinjiang's CSP geographical potential may be conservative, suggesting that the actual potential could be significantly higher. Overall, the suitability evaluation method proposed in Section 2 provides an effective analysis of regional adaptability. The final evaluation results can serve as a valuable reference for the site selection of power plant projects in the industry.

3.2.2. Analysis of technical potential results

As demonstrated in Table 6, the calculated results reveal that Tibet, Qinghai, Gansu, Xinjiang, and Inner Mongolia stand out as regions with the most abundant CSP generation potential, collectively accounting for over 60 % of the national CSP generation potential. Additionally, the regions of Heilongjiang, Jilin, Ningxia, and Liaoning also exhibit considerable development potential, accounting for 5.4 % in total. To further underscore the significant development potential of CSP, a comparison was conducted between the CSP generation and installed capacity potentials with the actual generation and installed capacity of CFP at present. The comparison results in Table 6 show that CSP generation in the high-quality generation resources areas (L4 and L5 regions) in Tibet, Qinghai, Gansu, Inner Mongolia, and Heilongjiang can entirely cover the current and future CFP generation in terms of power generation and installed capacity. Even in provinces like Xinjiang and Inner Mongolia, which have substantial CFP generation capacity, the high-quality CSP generation potential (in L4 and L5 regions) is respectively 19.79 times and 57.92 times the current generation capacity.

From a comprehensive national perspective, China's total electricity generation and installed capacity in 2023 were 9.2241 trillion kilowatt-hours and 2.92 billion kilowatts, respectively. Focusing on tower-type CSP, the high-quality generation resources available in just the four northwestern provinces alone have the potential to produce 6.12 times the current total national electricity generation. Expanding this view to the national level, the total generational potential of CSP in China is estimated to be between 7.58 and 18.22 times the current national generation. Furthermore, the potential installed capacity of tower-type CSP could amount to 28.27 times the present national total. These findings underscore the substantial development potential of CSP in China, highlighting its crucial role in the transition towards a future low-carbon power system. Such potential positions CSP not merely as an alternative energy source but as a key driver in China's strategic energy planning and sustainability goals.

3.2.3. Analysis of economic potential results

Based on the calculation method presented in Section 3.1.3, the spatial distribution of the LCOE for CSP and CFP in China is depicted in Fig. 14. The LCOE distribution features of CSP closely aligns with the

Table 6
Calculation and analysis results of CSP technical potential.

Province	CFP_{PG} in 2023 (10^3 GWh)	CFP_{IC} in 2023 (GW)	Level 5		Level 4		Level 3		Level 2		Level 1	
			R_{PG}	R_{IC}	R_{PG}	R_{IC}	R_{PG}	R_{IC}	R_{PG}	R_{IC}	R_{PG}	R_{IC}
Tibet	0.39	0.42	161e2	256e1	430e2	745e1	750e1	151e1	111e1	289.10	33.76	14.70
Qinghai	16.03	3.97	99.09	84.94	438.91	399.56	460.87	466.93	85.63	142.09	0.30	5.98
Gansu	103.86	25.25	5.65	4.79	35.38	32.17	49.44	65.48	12.86	28.21	0.08	0.60
Inner Mongolia	593.50	118.29	2.87	3.18	55.05	64.15	46.46	57.81	5.17	7.98	0.05	0.15
Xinjiang	378.96	66.56	1.11	1.37	18.68	23.16	20.22	31.46	9.82	26.93	0.21	2.14
Heilongjiang	93.57	25.57	2.12	1.84	51.43	46.30	47.41	79.80	1.63	5.35	0.00	0.03
Jilin	71.25	18.90	0.27	0.24	28.12	26.05	20.00	35.55	0.22	2.79	0.00	0.00
Ningxia	171.85	33.13	0.00	0.00	0.19	0.27	1.73	7.11	0.16	3.81	0.00	0.00
Liaoning	134.62	38.56	0.00	0.00	0.33	0.29	1.85	5.33	0.12	1.25	0.00	0.00

Notes: PG: power generatio; IC: installed capacity; R: ratio; R_{PG} = potential CSP_{PG} / practical CFP_{PG}; R_{IC} = potential CSP_{IC} / practical CFP_{IC};

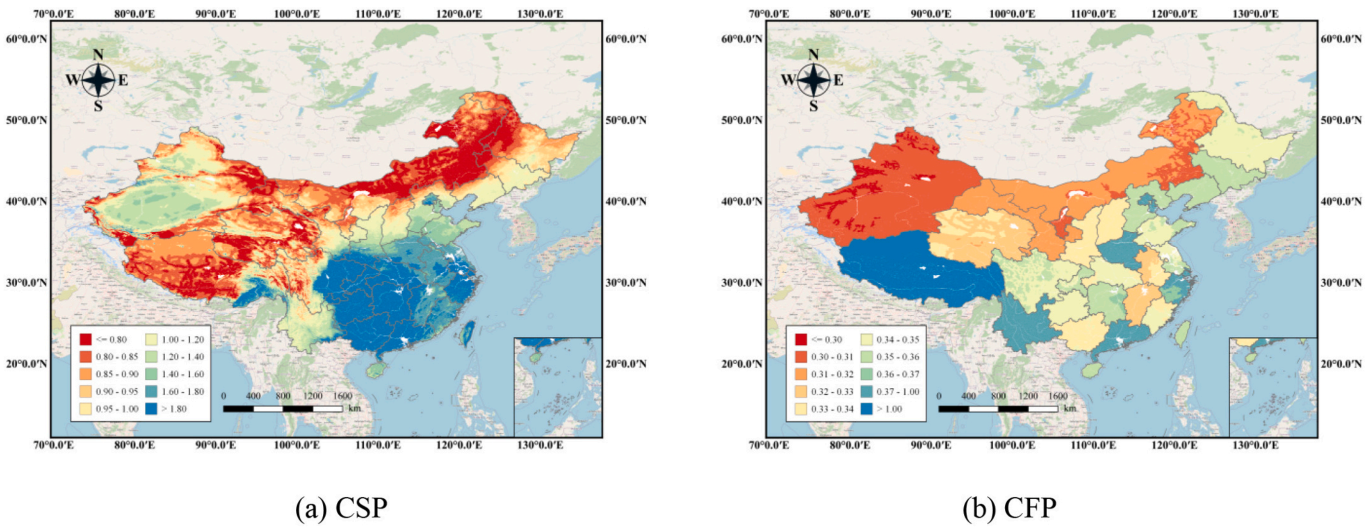

Fig. 14. LCOE maps for CSP and CFP.

distribution characteristics of DNI, as solar irradiance directly governs the power output of CSP stations. It is evident that regions with lower CSP generation costs align with the potential analysis results previously mentioned, predominantly concentrated in the northwestern region of China. In these regions, the LCOE of CSP generally ranges between 0.7 and 0.9 CNY/kWh. In areas with better resources, such as Gonghe in Qinghai, Jiuquan in Gansu, and Hami in Xinjiang, the LCOE can be as low as 0.68 CNY/kWh. Besides, a validation analysis, as shown in Table B8 of the supplementary material, of the LCOE calculations based on practical operational data and construction information is conducted to demonstrate the effectiveness of the proposed LCOE calculation model.

In the case of CFP generation, the impact of coal resource distribution on generation costs is somewhat mitigated, considering China's robust transportation network and distinctive electricity transmission pattern characterized by "West-to-East Electricity Transfer" and "North-to-South Electricity Transfer". As shown in Fig. 14 (b), the overall generation costs of CFP are significantly influenced by the annual generation hours of each province, exhibiting pronounced provincial characteristics. In the central and northeastern regions, including 14 provinces such as Hubei and Jiangsu, the LCOE is around 0.35 CNY/kWh. However, in the northwestern regions like Xinjiang, Inner Mongolia, and Ningxia, which benefit from both resource and policy advantages, resulting in higher annual generation hours, the LCOE is lower, with the average in Xinjiang as low as 0.303 CNY/kWh. In contrast, in the Tibet region, due to its limited geographical conditions and fragile ecological environment which are unsuitable for traditional CFP generation, the costs are exceptionally high.

Fig. 15 presents a comparative analysis of the LCOE spatial distribution for CSP and CFP across China. Nationwide, the cost of CFP is

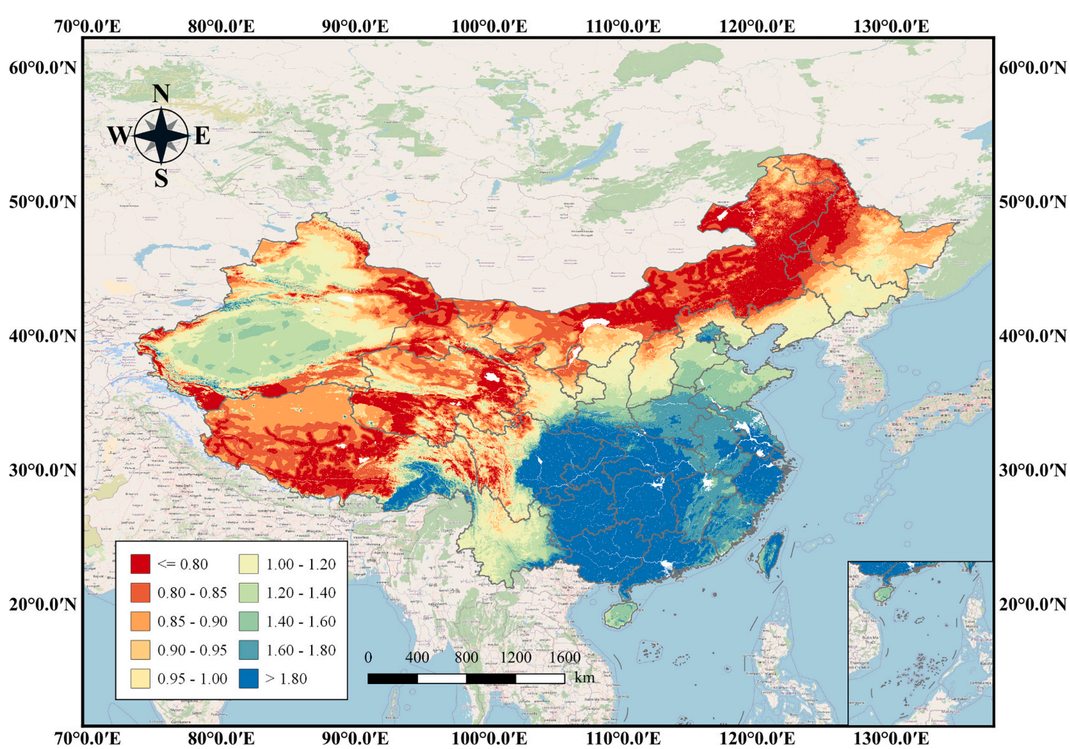

Fig. 15. LCOE comparison between CSP and CFP.

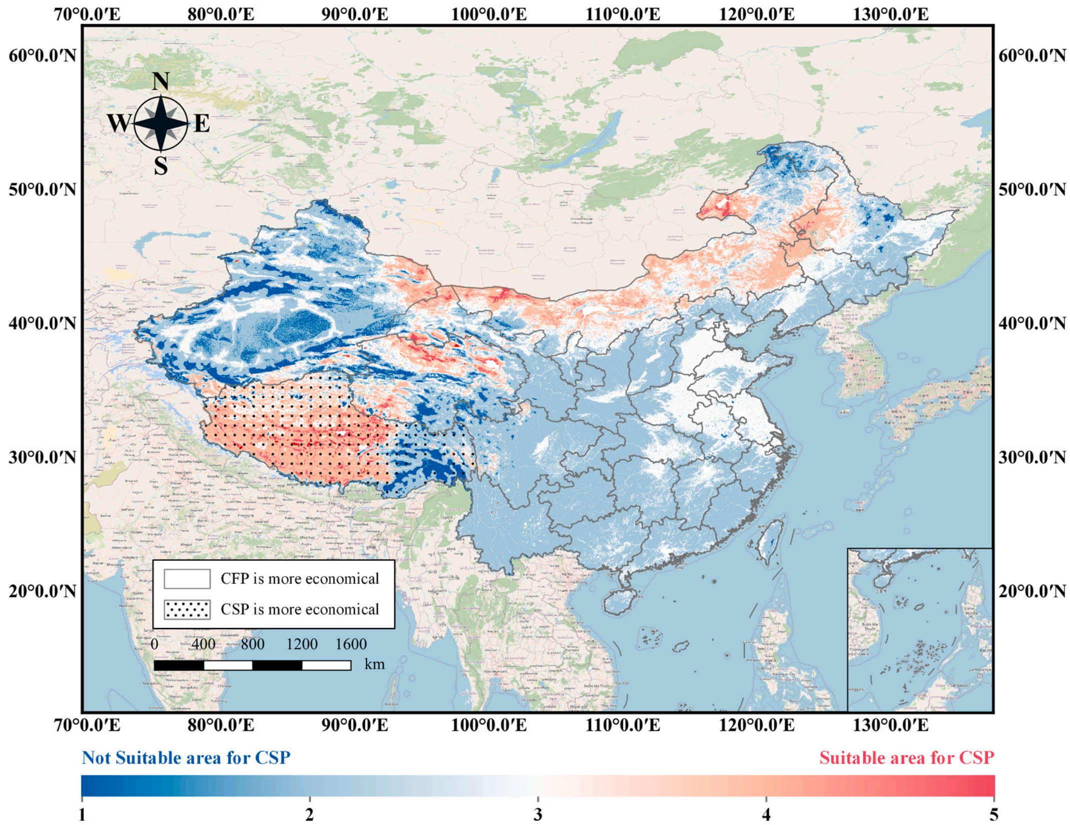

Fig. 16. Economically advantageous and technically feasible areas for CSP

generally lower than that of CSP. Particularly in the central, southern, and eastern regions, the LCOE of CFP is over 80 % lower than that of CSP. In the northern and northwestern regions, CSP costs remain more than 60 % higher than CFP, with CSP showing competitive costs only in areas with extremely abundant solar resources. Notably, in the Tibet region, CSP holds a distinct advantage from the standpoint of generation costs alone. According to Fig. 16, the data analysis shows that the area where standalone CSP is cost-competitive with CFP covers 1.07 million km^2, primarily concentrated in Tibet (excluding Shannan). Among these areas, the regions where CSP holds an economic advantage and is suitable for construction reaches 237,030 km^2, accounting for 11.51 % of the total geographically available area. In Inner Mongolia, Qinghai, Xinjiang, and Gansu, CSP, despite being technically feasible, still has relatively high construction costs for standalone plants. This significantly restricts the large-scale promotion of CSP, making the standalone replacement of CFP economically unfeasible.

4. Potential comparison of hybrid CSP-PV systems versus hybrid CFP-Wind systems

4.1. Overview

The findings delineated in Section 3 of this study suggest that CSP exhibits considerable potential for development within China, particularly in the northwest region where it possesses the capacity to supplant CFP both in generation and installation capabilities. However, the cost benefits of CSP, when compared with CFP, are not markedly pronounced. The high cost associated with CSP remains a major obstacle hindering its broader commercial adoption. Consequently, there emerges an exigent need for an innovative developmental strategy in the industry, one that effectively overcomes the cost barriers intrinsic to CSP.

In this context, the hybrid power generation technology integrating PV and CSP has garnered significant interest as a viable alternative. This methodology exhibits unique benefits, primarily in two aspects: Firstly, the exceptional peak-shaving capacity of CSP contributes to a consistent and stable output from the hybrid CSP-PV system. This characteristic notably reduces the influence of PV fluctuations on the power grid. Secondly, the synergistic integration of PV and CSP technologies facilitates the comprehensive harnessing of regional solar energy resources. This integration results in enhanced overall power generation efficiency and a consequent reduction in LCOE [136–141].

Conversely, while CFP currently maintains a cost advantage, it faces significant environmental challenges due to its high carbon emissions. Addressing these environmental concerns, scholars proposed a transition strategy tailored to Chinese contexts in the 2010s, termed the “Wind-Fire Bundle” [142], [143]. This strategy, when compared to projects of equivalent capacity employing CFP, not only substantially reduces the carbon emissions of the entire project but also improves the integration level of wind energy. In light of these considerations, this study engages in a comparative analysis of the two aforementioned hybrid systems — the CSP-PV hybrid and the CFP-Wind hybrid. This comparison is conducted from the perspectives of both land suitability and LCOE analysis, offering a comprehensive understanding of the relative advantages of each approach.

4.2. Methodologies for assessing potentials of hybrid generation systems

4.2.1. Assessing hybrid geographical potential

Currently, there is a scarcity of research on the suitability analysis of hybrid generation systems. Reference [104] represents a pioneering effort in this domain. In their approach, the authors have employed the land suitability analysis method, originally devised for CSP, and adapted it for the analysis of hybrid CSP-PV plants. This adaptation involves a combined application of the evaluation criteria for both CSP and PV. However, there are several issues with this methodology: 1) In the realm

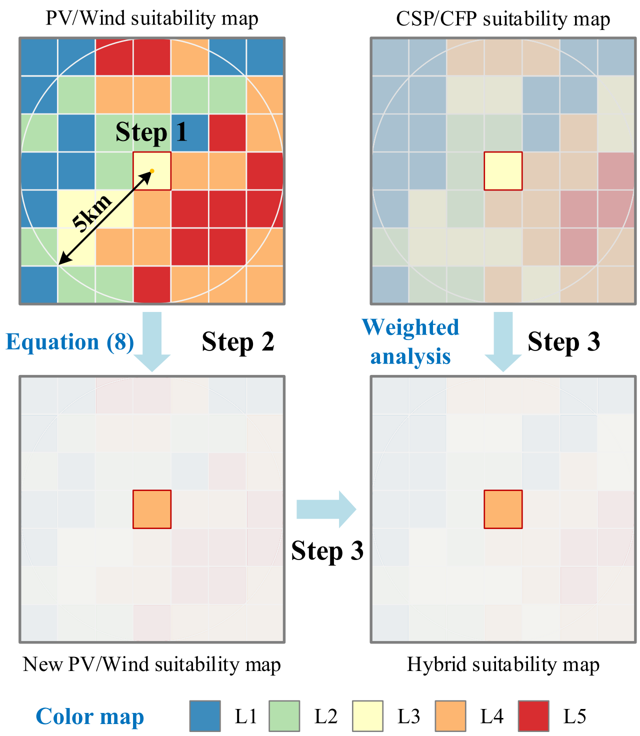

Fig. 17. Hybrid suitability analysis procedures

of practical engineering, CSPPs and PV plants within a joint power generation system are not necessarily situated in proximity to each other. Often, distances between these plants can surpass 5 km [144], [145]. This distance substantially exceeds the dimensions of most raster systems, rendering the analysis of such plants within a single raster point impractical. 2) CSP and PV, while both are forms of solar power generation, have distinct site requirements. A notable example is the significantly higher slope requirements for CSP. The application of a uniform set of evaluation criteria to both can yield excessively conservative outcomes. Furthermore, these challenges are further exacerbated when conducting joint suitability analysis for projects that integrate both wind and CFP power.

Considering the aforementioned factors, this paper proposes a novel methodology, based on practical engineering principles, for analyzing the land suitability of hybrid power generation plants. The proposed method, as depicted in Fig. 17, encompasses three primary steps: selecting a central generation type and establishing a buffer zone, re-evaluating the land suitability levels of non-central generation types, and calculating the overall suitability levels for hybrid generation. Firstly, the paper selects the generation type with more stringent selection criteria or higher construction costs as the central generation type, specifically CSP and CFP in this context. Subsequently, for the non-central generation types (i.e., PV and wind power), a 5 km radius buffer zone is created around each raster point on their respective suitability maps. Secondly, Eq. (8) is then used to determine the suitability levels for constructing PV/wind installations within these defined zones. As outlined in Fig. 17, Step 2, the new PV/Wind suitability is calculated as Level 4 in this example. Finally, a weighted analysis of the suitability maps for CSP/CFP and PV/Wind is conducted within the same raster cell. For example, according to Fig. 17, Step 3, the known CSP/CFP suitability level (Level 3) and the newly calculated PV/Wind suitability level (Level 4) are each weighted equally at 50 % within the raster cell. This yields a hybrid suitability level of Level 4 for the hybrid power plant within that raster cell. By applying this approach to every raster cell, comprehensive land suitability maps for various hybrid generation configurations are obtained.

$$Level_{suitability.new} = \left\lceil \frac{1^{*}N_{L1} + 2^{*}N_{L2} + 3^{*}N_{L3} + 4^{*}N_{L4} + 5^{*}N_{L5}}{N_{sum}} \right\rceil \tag{8}$$

4.2.2. Assessing hybrid economic potential

The LCOE methodologies for PV, wind, and CSP systems have reached a mature stage of development. In contrast, the analytical framework for hybrid LCOE remains nascent. Current research predominantly centres on contrasting the LCOE across various hybrid power generation technologies, or it delves into the temporal development trend of hybrid LCOE within specified, geographically fixed scenarios. However, investigations into the spatial distribution patterns of hybrid LCOE are relatively rare [29], [104].

To bridge the existing gap in the literature, this study proposes an enhanced model for hybrid LCOE analysis, building upon the foundational LCOE model proposed by Hernández-Moro et al. [19]. As illustrated in Fig. 18 and Eq. (9), the methodology for calculating the LCOE of hybrid power stations primarily adheres to the conventional approach of dividing the total lifecycle costs by the total electricity generation. However, in our model, the computation of total costs uniquely incorporates additional factors such as GDP and regional land prices, as detailed in Section A6-A7 of the supplementary material. Moreover, the estimation of total electricity generation in this paper not only accounts for the influence of spatial factors related to natural resources but also considers the impact of region-specific CSP development policies in China. This includes the assessment of typical capacity ratios between CSP and PV in different provinces, thereby examining the effects of varying degrees of hybridization in mitigating the renewable energy curtailment rates. For more calculation details, please refer to Section A8.

This comprehensive analysis significantly advances our understanding of the spatial distribution attributes of hybrid LCOE, specifically tailored to CSP-PV and CSP-Wind configurations. The inclusion of economic and policy considerations in the model provides a more holistic approach to evaluating the cost-effectiveness of hybrid renewable energy systems, offering valuable insights for policymakers and stakeholders in the renewable energy sector.

$$LCOE = \frac{C_{initial\_CSP} + C_{initial\_PV} + \sum_{n=0}^{N}\left(\left(C_{annual\_n\_CSP} + C_{annual\_n\_PV}\right)(1+r)^{-n}\right)}{\sum_{n=0}^{N}\left(\left(E_{n\_CSP} + E_{n\_PV}\right)(1+r)^{-n}\right)} \tag{9}$$

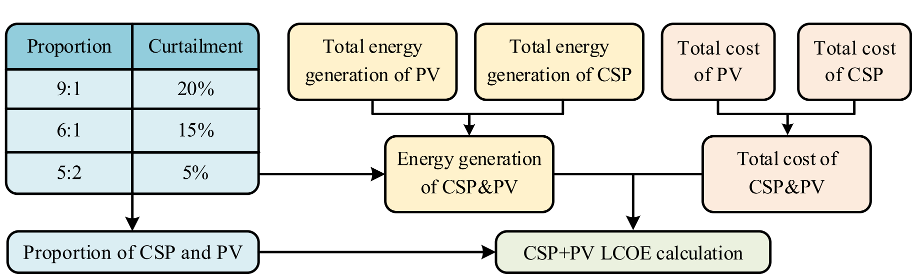

Fig. 18. Hybrid LCOE calculation procedures of the CSP-PV system.

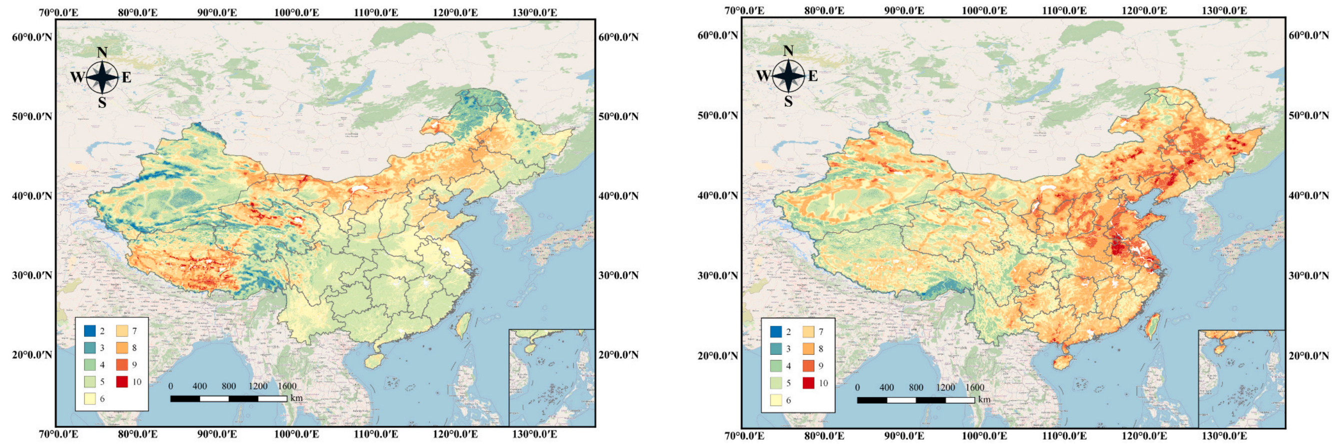

(a) Hybrid CSP and PV

(b) Hybrid CFP and Wind

Fig. 19. Land suitability map for hybrid generation systems.

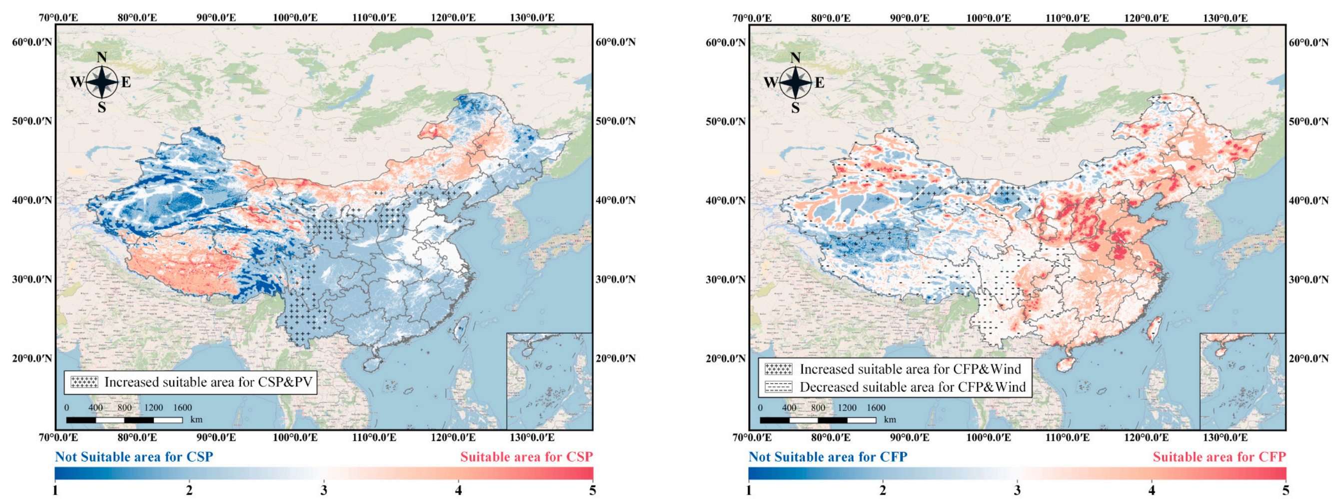

(a) CSP vs. hybrid CSP-PV

(b) CFP vs. hybrid CFP-Wind

Fig. 20. Comparison of changes in suitable areas for single and hybrid generation systems

4.3. Analysis of results for hybrid generation systems

4.3.1. Analysis of hybrid geographical potential results

To conduct the geographical potential analysis for hybrid renewable energy, this study adopts a method similar to Section 3.1.1, evaluating land suitability for PV and Wind respectively. Further details are available in Section A7-A9 of the Supplementary material. Building on this foundation, the study then utilizes the analytical approach introduced in Section 4.2.1 to further comprehensively examine the land suitability of hybrid PV and CSP technologies. The results, illustrated in Fig. 19 (a) and Fig. 20 (a), reveal that the area of high-quality regions (level 6 and above) for hybrid CSP-PV across the nation has increased by 19.79 % over CSP alone, indicating that integrating PV significantly expands viable areas for CSP, providing a substantial positive impetus for the promotion of CSP technology. Conversely, the area of high-quality regions (level 6 and above) for hybrid CFP-Wind across the nation has decreased by 8.93 %. This decrease is primarily due to the fact that CFP and wind are not similar resources, and the differences in their resource distributions limit the application range of this hybrid generation.

Regionally, hybrid PV-CSP technologies notably improve the competitiveness of CSP against CFP, especially in the Northwest and Southwest, as depicted in Fig. 21. Specifically, in the Southwest region, the proportion of areas with comparative advantages increased from 37.11 % in standalone CSP systems to 46.61 % in hybrid CSP-PV systems, representing a significant rise of nearly 10 %. Moreover, areas like Gansu and Qinghai saw over a 20 % increase in advantageous regions with hybrid technology, while in wind-dominant provinces like Heilongjiang, Jilin, and Inner Mongolia, the trend for CSP advantageous areas decreased, highlighting the varied impact of hybrid systems across different regions.

Furthermore, to further substantiate the reliability of the proposed analytical method, this study undertook case studies of operational hybrid power stations spanning a diverse array of geographic regions within the nation. As illustrated in Table 7 and Table 8, a comparative analysis between actual satellite maps and geographical potential maps reveals that the existing hybrid power stations are all located in areas with land suitability of level 8 or higher. This finding affirmatively

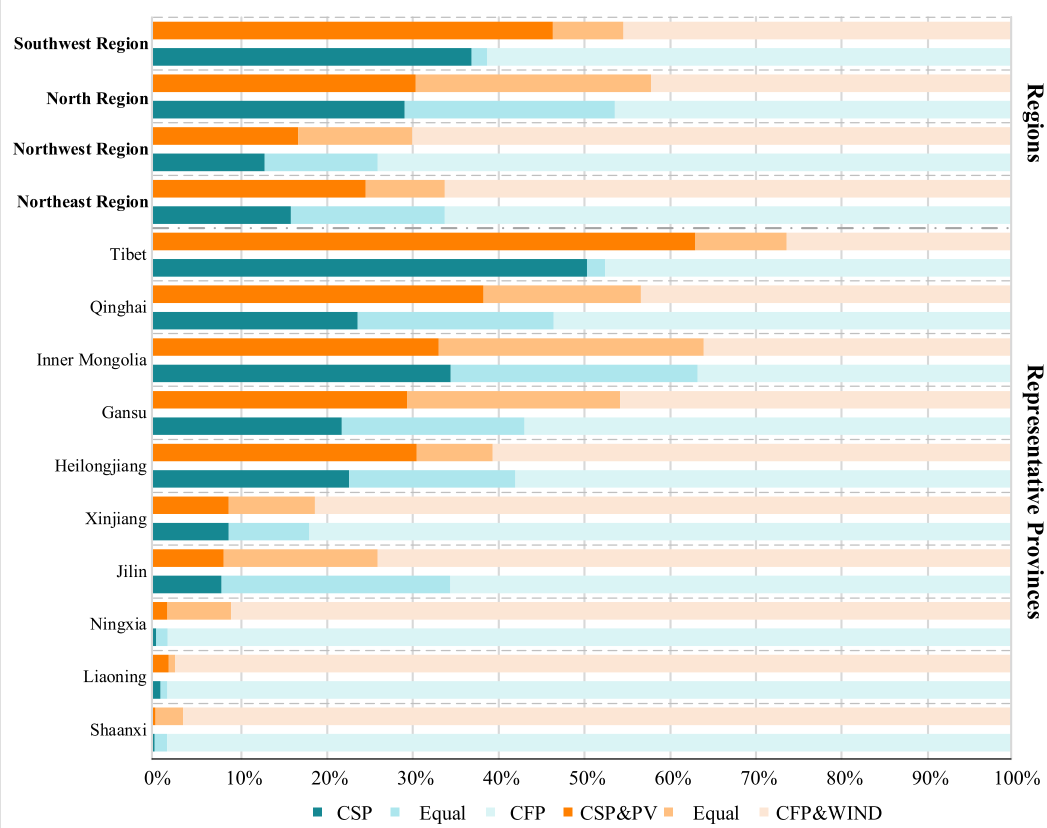

Fig. 21. Land suitability comparison between two hybrid generation systems.

Table 7
Comparative case analysis between potential map and satellite map for hybrid CSP-PV systems.

Label	(1)	(2)	(3)	(4)	(5)
Location	Dunhuang, Jiuquan, Gansu	Delingha, Haixi Zhou, Qinghai	Yiwu, Hami, Xinjiang	Akesai, Jiuquan, Gansu	Gonghe, Hainan Zhou, Qinghai
Potential map	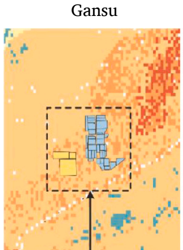	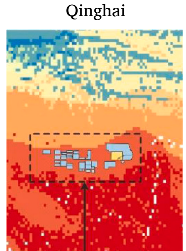	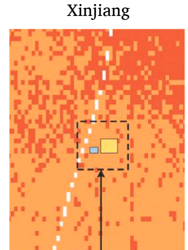	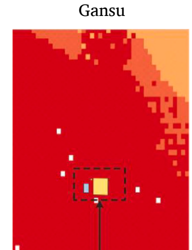	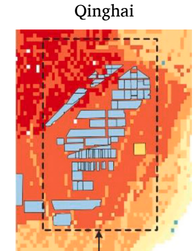
Satellite map	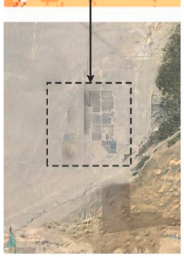	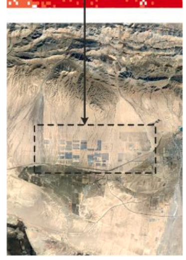	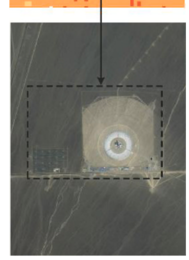	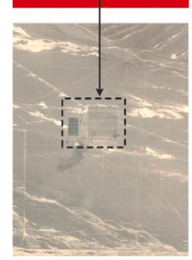	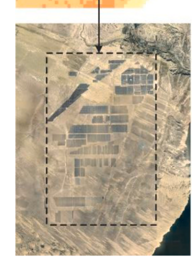

Table 8
Comparative case analysis between potential map and satellite map for hybrid CFP-Wind systems.

Label	(1)	(2)	(3)	(4)	(5)
Location	Zhenglan Banner, Xilin Gol League, Inner Mongolia	Huolin Gol, Tongliao, Inner Mongolia	Ulanhot, Xing'an League, Inner Mongolia	Mile, Honghe, Yunnan	Dabancheng, Urumqi, Xinjiang
Potential map	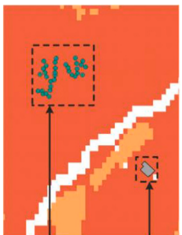	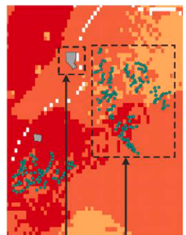	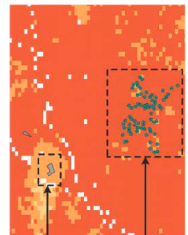	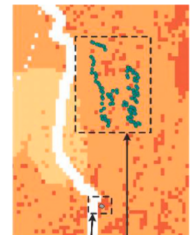	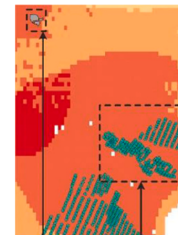
Satellite map		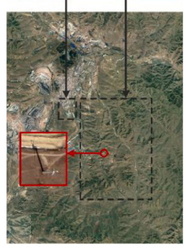			

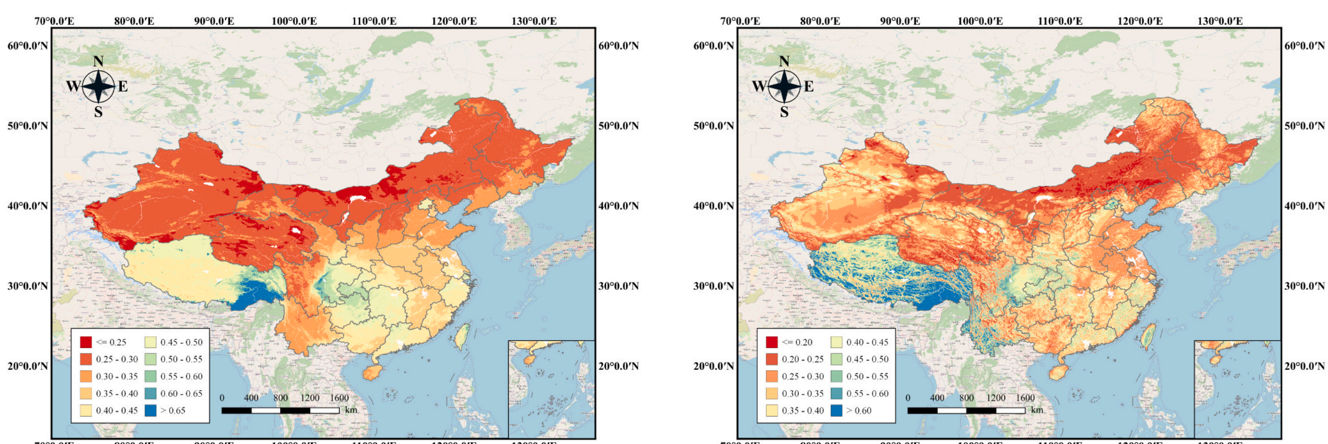

(a) Hybrid CSP and PV

(b) Hybrid CFP and Wind

Fig. 22. LCOE for hybrid generation systems.

corroborates the methodological soundness and validity of the proposed land suitability analysis technique for hybrid power generation systems. Additionally, the cases selected for validation are derived from a broad spectrum of provinces, namely Gansu, Qinghai, Xinjiang, and Inner Mongolia, encompassing diverse landscapes including deserts, mountains, and rivers. This extensive and varied dataset not only attests to the method's applicability across different topographical and ecological scenarios but also significantly highlights the robustness and adaptability of the proposed analytical approach.

1.1.1 *Analysis of hybrid economic potential results*

According to the methodology described in section 4.2.2, the spatial distribution of the LCOE for the hybrid CSP-PV system and hybrid CFP-Wind system is depicted in Fig. 22. Comparative analysis with the LCOE of individual generation technologies, as illustrated in Fig. 14, reveals that integrating the cost and applicability advantages of PV and wind results in a nationwide reduction of LCOE for both hybrid generation systems. This reduction substantially enlarges the area where the construction of hybrid energy systems is economically viable. Particularly, the LCOE for the hybrid CSP-PV system, in contrast to the generally higher construction costs associated with standalone CSP technology—predominantly situated at 0.8 CNY/kWh—has witnessed significant reductions in provinces such as Qinghai, Inner Mongolia, Gansu, Xinjiang, Ningxia, and Heilongjiang. In these regions, the cost has been reduced to below 0.3 CNY/kWh, spanning an extensive area of 4.6 million km^2. Additionally, the LCOE for these hybrid generation systems highlights the complementary characteristics of the integrated technologies, thereby lessening the influence of policy disparities across provinces and regions. For instance, the hybrid CFP-Wind system demonstrates that while the LCOE of standalone CFP exhibits pronounced provincial variations, the inclusion of wind energy tends to obscure provincial boundaries in the LCOE distribution for the hybrid system, though it accentuates intra-provincial differences.

From the perspective of CSP's economic substitutability, the area where standalone CSP is cost-competitive with CFP covers only 1.07 million km^2. In contrast, the area where the LCOE of the hybrid CSP-PV system is lower than that of the hybrid CFP-Wind system expands to 3.5 million km^2 (according to Fig. 23), marking an increase of 226.19 %. Notably, in vast regions of Qinghai and Tibet, the Hexi Corridor in Gansu, and the northwestern parts of Xinjiang, the LCOE of hybrid CSP-PV system, with an average price as low as 0.277 CNY/kWh, is over 30 % lower than that of hybrid CFP-Wind system. In areas like Inner Mongolia and the Northeastern region, owing to the favourable economic and technical feasibility of both technologies, the LCOE in 48.97 % of the regions are comparably well-aligned. However, in the Central, Eastern, and Southern regions of China, the cost benefits of the hybrid CFP-Wind system markedly dominate in 86.49 % of the areas. The combined technical and economic analysis results in Fig. 24 indicate that the areas where the hybrid CSP-PV system is economically advantageous and technically feasible (with a geographical potential rating above level 5) cover a total of 585,020 km^2. These areas are primarily distributed in northern and central Qinghai, the Hami region in eastern Xinjiang, northern and central Tibet, and parts of Ejin Banner and Alxa Right Banner in Inner Mongolia, accounting for 28.40 % of the total geographically available area.

5. Discussion

5.1. Sensitivity analysis

5.1.1. Effects of technological advances on CSP's economic viability

According to the technical comparison analysis presented in Section 2.2, CSP and CFP exhibit similar backend structures. However, modern CSP projects predominantly utilize molten salts as mediums for heat storage and transfer, with operational temperatures peaking at 600 °C and typically employing subcritical cycles. These factors contribute to a notable disparity in cycle efficiency between CSP and CFP. Consequently, the exploration of new heat transfer fluids and the adoption of innovative power generation cycles are critical pathways for CSPPs to enhance overall power generation efficiency and reduce operational costs. As depicted in Fig. 25, when the system's overall efficiency approximates 35 %, the cost of CSP in the key regions hovers around 0.5 CNY/kWh. In resource-rich areas, these costs have even approached the current average costs associated with CFP. Furthermore, computational analysis indicates that an increase in CSP efficiency to 35 % expands the economically viable area for CSP to replace CFP by over 10 %, thereby improving the economic viability of substituting CFP with CSP.

5.1.2. Effects of CSP-PV capacity ratios on hybrid geographic potential

In Section 4.2, the land suitability analysis for hybrid CSP-PV plants employs a balanced weighting approach, assigning an equal 50 % importance to both PV and CSP technologies, underscoring their comparable significance from a technical standpoint. However, in operational hybrid CSP-PV plants, the capacity ratios for CSP typically vary as follows: 10 % (1:9), 14.29 % (1:6), or 28.57 % (2:5), indicating that PV has a greater influence from the perspective of capacity ratio. Consequently, this section examines how different CSP capacity ratios directly affect the outcomes of geographic potential analysis for hybrid CSP-PV systems when the analysis is predominantly based on these capacity ratios. According to Fig. 26, as the proportion of CSP capacity decreases,

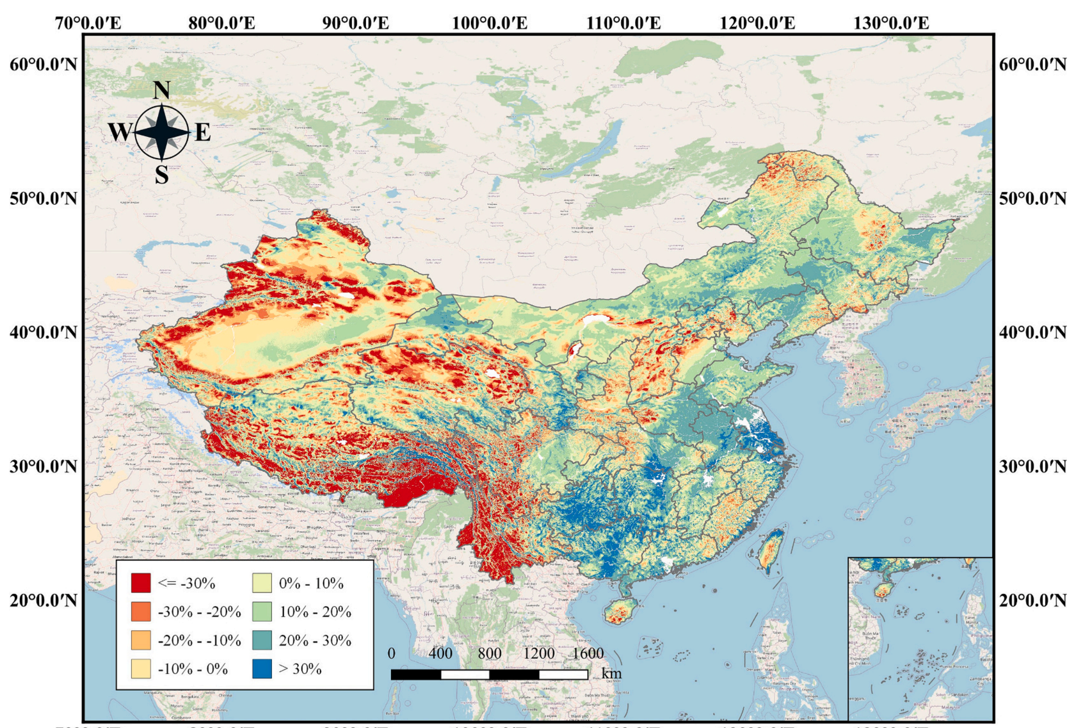

Fig. 23. LOCE comparison between two hybrid generation systems.

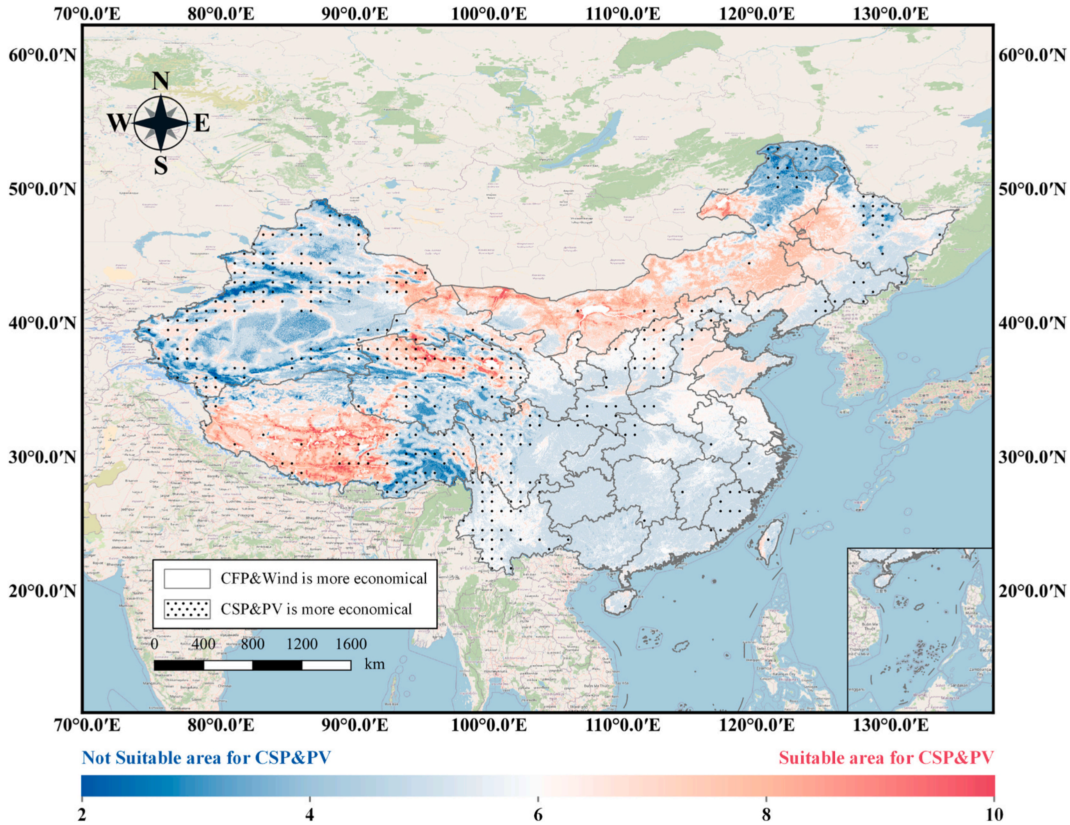

Fig. 24. Economically advantageous and technically feasible areas for hybrid CSP-PV systems

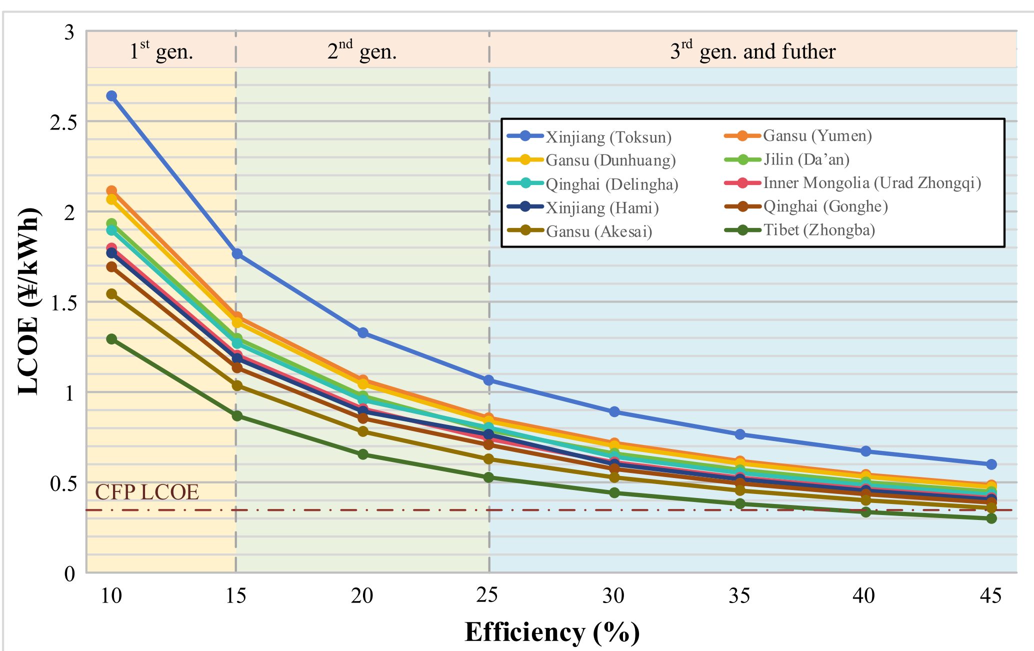

Fig. 25. Impact of efficiency on CSP's LCOE.

there is a corresponding increase in the proportion of areas rated with higher potential levels. This trend occurs because PV, compared to CSP, requires less stringent geographical conditions concerning slope, sunlight, and water resources, which enhances its overall adaptability. Therefore, when PV has a more dominant role within the hybrid configuration, the geographic potential analysis results for hybrid power generation are more favourable. This finding suggests that the analysis results presented in this document are conservative; in practical applications, the land suitability outcomes for hybrid CSP-PV systems are likely to be even more advantageous.

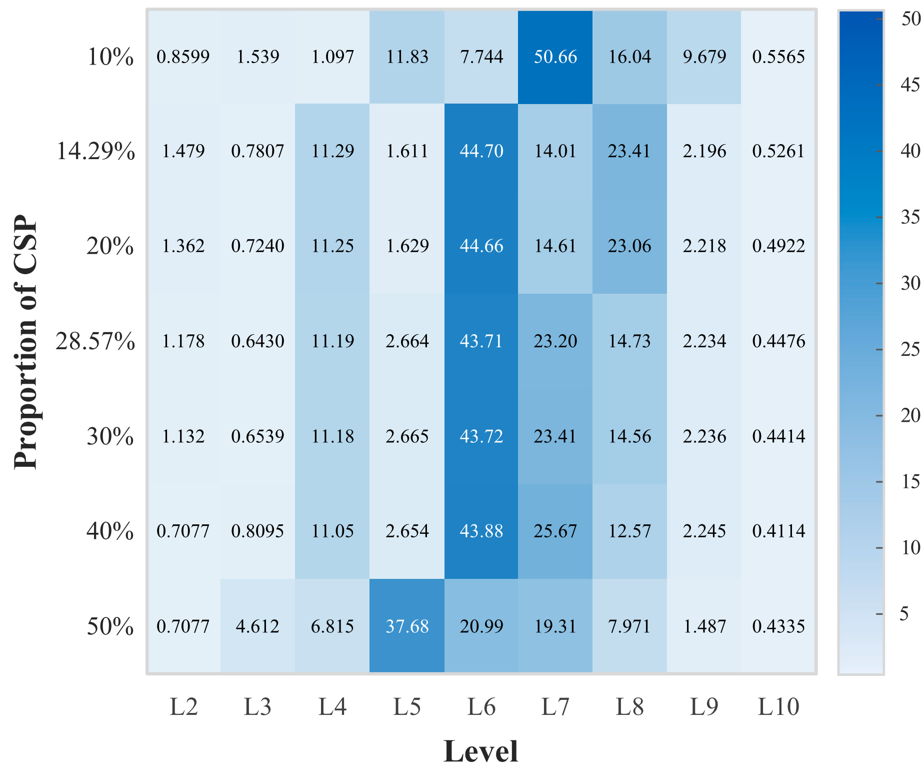

Fig. 26. Impact of CSP weighting ratios on the geographic potential of hybrid CSP-PV systems

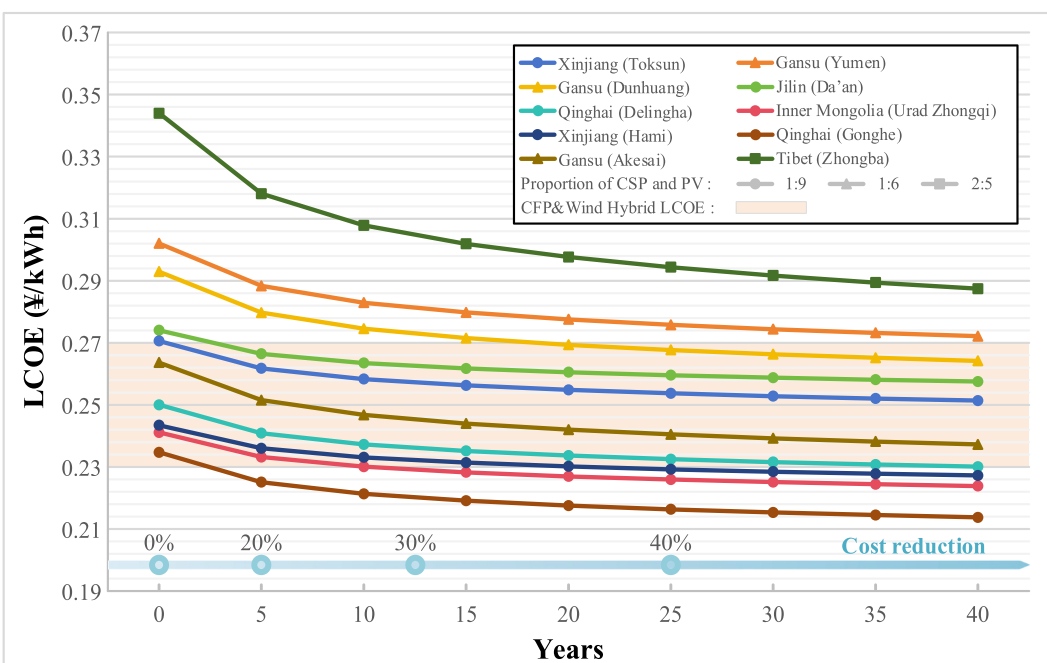

Fig. 27. Impact of industry scaling on the LCOE of hybrid CSP-PV plants

5.1.3. *Effects of industry scaling on hybrid CSP-PV plant costs*

In contrast to CFP, the industry volume of CSP is rapidly and robustly expanding, with significant room for cost reduction through scaling. In this section, the CSP learning curves from [19] are applied to analyze the impact of CSP industry scaling on the cost reduction of hybrid CSP-PV plants. As shown in Fig. 27 this section selects ten geographically representative locations to analyze the cost trends under different CSP proportions. It is observed that as CSP scales and its supply chain matures, the LCOE of hybrid CSP-PV plants is expected to decrease substantially over the next five years. This reduction is particularly notable in regions with a high proportion of CSP, such as Tibet. Simultaneously, as the supply chain matures, the LCOE of hybrid CSP-PV plants in advantageous locations in Qinghai, Xinjiang, and Inner Mongolia are beginning to align with those of hybrid CFP-Wind plants. Nevertheless, as the industry scale reaches a certain level, its impact on reducing the costs of CSP generation diminishes. Therefore, it is crucial to simultaneously advance supply chain development and continuous technological innovation to jointly drive a rapid reduction in CSP costs.

5.2. Policy recommendations

Based on the findings from Sections 3 and 4, it is evident that while CSP-PV hybrid generation technologies can somewhat mitigate the high construction costs associated with CSP projects, the costs of standalone CSP systems remain considerably higher than those for CFP generation. Additionally, the withdrawal of national subsidies in 2021 has led to diminished investment returns for CSP projects, and the market scale for CSP is still relatively small. In the absence of sustained policy support, the viability of CSP projects is at risk. Therefore, it is crucial to implement effective measures to reinforce industry confidence, foster the healthy growth of the CSP sector, and increase the feasibility of CSP as an alternative to CFP. This section offers targeted policy recommendations from three perspectives—industry advancement, technological innovation, and market development—integrating insights from previous analyses with real-world industry challenges.

5.2.1. Fostering industry advancement

5.2.1.1. Prioritizing strategic site selection and development. Geographic, technological, and economic advantages for CSP are concentrated in northern, northwestern, and Tibetan regions, which should be prioritized for development and promotion to stimulate the growth of CSP technologies and the industry supply chain, thereby reducing costs. Under the incentive policies for large desert bases, it is advisable to prioritize the development of CSP in regions with advantageous conditions to drive technological advancements in the CSP industry. Additionally, some land should be reserved for CSP construction in areas designated for large-scale centralized photovoltaic projects, ensuring space for future CSP development and expansion.

5.2.1.2. Optimizing CSP power station construction. The main challenges in CSP construction involve the ratio of mirror fields to installed capacity. Currently, for integrated multi-energy projects including CSP, the benchmark electricity price of CFP is insufficient to recoup investment costs, forcing investors to significantly reduce the scale of CSP's solar field. This reduction compromises the electricity generation capacity and flexibility of CSP, losing the long-duration storage technological advantage. Therefore, policies are urgently needed to set thresholds for the configuration of the solar field, thus enhancing the regulatory capabilities of CSPPs and guiding the sustainable development of the industry. Additionally, in current large renewable energy-based projects, the installed capacity of CSP is constrained by the economics of grid parity. The role of CSP is defined as a "peak-shaving power source," with a relatively low-capacity ratio (often 1:6 or 1:9), which is not the optimal mix for economic and stability considerations. Thus, optimal CSP capacity ratios should be determined for each power station based on actual site selection, local resource advantages, grid structure, and consumer demands.

5.2.1.3. Enhancing the CSP supply chain. Through the construction of demonstration projects, China has established a comprehensive CSP equipment manufacturing industry chain, with some power stations achieving international leadership in design, construction, and operation. However, the high investment costs and small scale of CSP projects limit market and technology iteration opportunities. Consequently, design, construction, and equipment standardization have lagged, hindering industry scale effects and rapid industry expansion. Policy incentives and support are recommended for critical industry segments to accelerate the development of key equipment and materials. Given the structural similarities between CSP and CFP outlined in Section 2, the CSP industry could utilize CFP's industrial resources to enhance its manufacturing system. Moreover, policies should encourage retrofitting operational and retired coal power plants with solar collection and storage devices to reduce fossil fuel use and enhance system flexibility. Ultimately, it is believed that under appropriate policy guidance, the transformation and upgrading of the CSP industry can be achieved concurrently with the smooth transition of the CFP sector.

5.2.2. Driving technological innovation

5.2.2.1. Funding and support for CSP technological advancements. Technological innovation serves as the cornerstone of industry progression. It is essential to accelerate foundational research and facilitate the development and demonstration of innovative CSP technologies. It is advisable for national initiatives and science and technology projects to allocate funding specifically for the research of pivotal and original CSP technologies, such as supercritical carbon dioxide thermoelectric technologies, high-temperature trough and tower CSP technologies at 600 °C, and integrated CSP and thermal power operations. To promote the swift implementation of these technologies, establishing incentive policies that encourage the execution of demonstration projects within CSP industrial parks is recommended.

5.2.2.2. Enhancing CSP efficiency and cost-effectiveness. In the current technological framework, optimization and innovation emerge as direct and effective strategies for cost reduction. Key areas for improvement in CSP technology using molten salt as a heat transfer medium include enhancing the efficiency of mirror fields, boosting equipment reliability, and optimizing operational and maintenance practices. Notably, leading CSP construction companies have already acquired substantial commercial experience and achieved noteworthy successes in these domains. Thus, it is crucial for the government to facilitate and promote technical exchanges and healthy competition among companies, fostering rapid technological iterations within the CSP industry to achieve significant reductions in costs and enhancements in efficiency.

5.2.2.3. Expanding CSP applications across various scenarios. CSP technology, which encapsulates the "light-heat-electricity" conversion processes, holds significant potential for diverse development applications, capable of simultaneously providing thermal and electrical energy. Development strategies should encourage the adaptation of CSP-based clean energy heating systems to local conditions, suitable for residential heating and industrial applications [146–149]. Moreover, given the rich energy mineral and rare metal resources in China's northwestern region, there is a vast potential for resource development. However, traditional grid-connected power supply models face challenges in this region due to harsh geographical conditions and high construction costs. A CSP-led off-grid power supply model offers a solution with high reliability, low costs, and environmental benefits. For instance, the successful operation of the Zabuye Salt Lake lithium extraction project in Tibet in 2023, the world's first high-altitude clean energy microgrid primarily powered by a CSP station, exemplifies the strategic utilization of CSP's intrinsic properties to actively promote its application across various scenarios.

5.2.3. Strengthening market infrastructure

Currently, CSP is in a transitional phase, predominantly serving as a regulatory power source within hybrid CSP-PV generations and large renewable energy bases. Operational strategies are tailored to peak during morning and evening high-demand periods, resulting in only approximately 2000 annual generation hours. Persisting with traditional benchmark pricing models not only undermines the economic returns of CSP but also fails to leverage its full functional potential [150–155]. Consequently, market reforms are imperative to revise the pricing mechanisms for CSP's grid integration, ensuring they reflect its substantial value in supporting and regulating the power system.

A suggested initiative is to pilot a “volume + capacity” pricing mechanism in the northwest’s extensive new energy bases, setting clear national compensation standards and regional fluctuation ranges for CSP capacity pricing. Additionally, enhancing the power auxiliary services market is crucial. This includes establishing robust mechanisms for peak regulation and frequency adjustment, and integrating CSP’s unique characteristics and technological pathways. Despite CSP’s recognition in auxiliary services, tailored policies are needed to formulate viable compensation and operational models that adapt to technological advancements and cost dynamics in the CSP sector.

Furthermore, the implementation of green certificates and green power trading schemes is essential to monetize the environmental benefits of CSP, promoting its sustainable development. As the power market framework and overarching policies continue to evolve, CSP’s competitive position in the electricity market will strengthen, leading to market-based pricing that not only secures its profitability but also enhances the overall system’s regulatory capabilities.

5.3. Future work

Beyond the primary scope of this study, several important points have emerged that necessitate further research. Firstly, this paper primarily evaluates the feasibility of CSP as a replacement for CFP in China from geographical, technical, and economic perspectives. However, it is also essential to analyze this feasibility from a power system perspective, particularly regarding flexibility and frequency security. This line of research is challenging due to the necessity of considering numerous factors, including external environmental conditions, multiple time scales, and varying degrees of substitution. For CSP itself, the temperature and storage volume of molten salt are influenced by weather and seasons, affecting its dynamic regulation performance. Therefore, analyzing and comparing CSP’s flexibility and frequency response capabilities under different weather and seasonal conditions across multiple time scales will help clarify the impact of CSP replacing CFP. For regional systems, the impact of different levels of CSP replacing CFP on system flexibility and frequency stability within a specific region is not yet clear and requires further research and practical engineering efforts.

Furthermore, the environmental and social impacts of CSP replacing CFP are worth exploring. Although CSP can reduce carbon emissions compared to CFP, the local ecological impacts of CSP are influenced by various factors, including plant scale, design form, and location. On the social impact side, CSP can inherit part of CFP’s downstream industrial chain and promote local employment and economic development. However, as most CSPPs are still in the planning and construction stages, the social impacts of large-scale substitution are not yet clear. Thus, exploring the environmental and social impacts of large-scale CSP substitution for CFP in actual scenarios is a challenging task that warrants further research and analysis. Third, a more accurate weighted analysis method is worth studying. Although the AHP method utilized in this study is sufficient for assessing CSP potential on a national scale, future research should explore more diverse hybrid subjective-objective weighting methods to mitigate the influence of subjective decision-making inherent in the AHP method, thus enhancing decision credibility and leading to more rational weight distribution.

6. Conclusion

CSP is a green, low-carbon, and stable power generation technology that offers both peak-shaving and energy storage capabilities, making it a potential replacement for CFP in some regions. However, the feasibility of CSP replacing CFP lacks systematic and scientific quantitative analysis and comparison. To address this, this paper conducts a detailed and in-depth comparative analysis of CSP and CFP, as well as hybrid generation models, from multiple perspectives, including industry development status, technological characteristics, and technological potential. This work can help determine the feasibility and limitations of CSP replacement strategies and clarify the future development positioning of CSP. The main findings are summarized below:

1) This paper compares the industrial and technological development status of CSP and CFP, focusing on installed capacity, policy support, structural characteristics, and technological development history. The comparison shows that CFP installations have decreased from 71.48 % in 2012 to 47.62 % in 2023, however, their electricity generation share remains above 65 %, indicating strong dependency. In contrast, China’s CSP capacity has grown from 0 to 588 MW in the past five years but remains negligible compared to CFP. On the policy front, China has implemented robust support measures for CSP, including demonstration projects, price subsidies, and research funding to promote its development. Conversely, policies towards CFP have become increasingly stringent, including strict regulations on new projects to reduce CFP’s share, enforcing international standards on new units for lower emissions, and promoting operational flexibility reforms.
2) This study evaluates the viability of CSP as a substitute for CFP from geographical, technical, and economic perspectives. Geographically, CSP has 2.06 million km^2 available for construction, roughly half of the 5.07 million km^2 suitable for CFP. Technically, CSP generation capacity in high-quality regions can meet and exceed current and future CFP demands, with the potential in some provinces being exponentially higher. The total generational potential of CSP in China is estimated to be 7.58 to 18.22 times the current national generation, with tower-type CSP installed capacity potentially reaching 28.27 times the present total. Economically, the LCOE for CSP is substantially higher than CFP across most regions, except in areas with abundant solar resources like Tibet, where CSP shows a cost advantage of over 1.07 million km^2. Regions where CSP is economically advantageous and suitable for construction cover 237,030 km^2, accounting for 11.51 % of the total geographically available area. Therefore, despite its promising technical feasibility and geographical potential, the high costs of standalone CSP hinder its large-scale substitution for CFP.
3) This study compares CSP-PV and CFP-Wind hybrid systems, focusing on suitability and LCOE analysis. Results indicate that the area of high-quality regions for hybrid PV-CSP increased by 19.79 % over CSP alone, enhancing CSP’s viability. Regionally, hybrid PV-CSP technologies improve CSP’s competitiveness, particularly in the Northwest and Southwest. For instance, the Southwest saw a rise from 37.11 % to 46.61 % in advantageous areas, while Gansu and Qinghai in Northwest regions experienced over a 20 % increase. Conversely, wind-dominant provinces like Heilongjiang, Jilin, and Inner Mongolia showed decreased CSP advantageous areas. Economically, the LCOE for hybrid CSP-PV systems has significantly decreased to below 0.3 CNY/kWh in several provinces, spanning 4.6 million km^2. The hybrid CSP-PV system covers 3.5 million km^2 where its LCOE is lower than the hybrid CFP-Wind system, marking a 226.19 % increase compared to standalone CSP. In regions like Qinghai, Tibet, and Gansu, the LCOE of hybrid CSP-PV is over 30 % lower than hybrid CFP-Wind. However, in Central, Eastern, and Southern China, the hybrid CFP-Wind system dominates in 86.49 % of areas. The combined analysis indicates that hybrid CSP-PV systems are economically advantageous and technically feasible over 585,020 km^2, primarily in northern and central Qinghai, eastern Xinjiang, northern and central Tibet, and parts of Inner Mongolia, accounting for 28.40 % of the total geographically available area.
4) This study utilized real power station data to validate the geographic potential results for both single and hybrid power technologies, confirming the reliability of the proposed potential assessment framework. Additionally, a sensitivity analysis is conducted to explore the effects of factors, including generation efficiency, CSP-PV capacity ratios, and industry scaling, on the results. Furthermore, integrating the comparative results with CSP development

challenges, this study proposes targeted policy recommendations to advance industry growth, spur technological innovation, and enhance market infrastructure.

CRediT authorship contribution statement

Lingxiang Yao: Conceptualization, Investigation, Methodology, Validation, Data curation, Formal analysis, Writing – original draft, Writing – review & editing. **Zhiwen Guan:** Writing – review & editing, Validation, Methodology, Investigation, Formal analysis, Data curation, Conceptualization. **Yang Wang:** Writing – review & editing, Visualization, Supervision, Project administration. **Hongxun Hui:** Resources, Supervision, Visualization, Writing – review & editing. **Shuyu Luo:** Writing – review & editing, Writing – original draft, Visualization. **Chuyun Jia:** Writing – review & editing, Visualization, Supervision, Resources. **Xingxing You:** Writing – review & editing, Visualization, Supervision, Resources. **Xianyong Xiao:** Writing – review & editing, Visualization, Supervision, Resources, Project administration.

Declaration of competing interest

The authors declare that they have no known competing financial interests or personal relationships that could have appeared to influence the work reported in this paper.

Data availability

Data will be made available on request.

Acknowledgements

This work was supported by the National Natural Science Foundation of China under Grant 52177104. The authors are grateful for the support provided by the engineers from Lanzhou Dacheng Technology Co., Ltd. and China General Nuclear Power Co., Ltd. Besides, in recognition of Guan Zhiwen's outstanding contributions, Dr. Yao is pleased to offer him co-first authorship.

Appendix A. Supplementary data

Supplementary data to this article can be found online at https://doi.org/10.1016/j.apenergy.2024.124396.

References

[1] IRENA. Renewable capacity statistics 2024. Abu Dhabi: International Renewable Energy Agency; 2024.
[2] IEA. Renewables 2023. Paris: International Energy Agency; 2024.
[3] IRENA. World Energy Transitions Outlook 2022. Abu Dhabi: International Renewable Energy Agency; 2022.
[4] Paris. Paris agreement. In: Report of the conference of the parties to the United Nations framework convention on climate change (21st session, 2015: Paris). Retrived December. HeinOnline; 2015, https://unfccc.int/sites/default/files/english_paris_agreement.pdf.
[5] Administration National Energy. The National Energy Administration releases national power industry statistics for 2023:2024.
[6] National Energy Administration. The National Energy Administration released the 2023 national power industry statistics. 2024.
[7] China Electricity Council. China electric power statistical yearbook 2023:2023.
[8] He Y, Qiu Y, Wang K, Yuan F, Wang W-Q, Li M-J, et al. Perspective of concentrating solar power. Energy 2020;198:117373.
[9] Zhuo Z, Du E, Zhang N, Nielsen CP, Lu X, Xiao J, et al. Cost increase in the electricity supply to achieve carbon neutrality in China. Nat Commun 2022;13:3172.
[10] Wang Z. Design of Solar Thermal Power Plants. Academic Press; 2019.
[11] Ferruzza D, Kærn MR, Haglind F. A method to account for transient performance requirements in the design of steam generators for concentrated solar power applications. Appl Energy 2020;269:114931.
[12] Baigorri J, Zaversky F, Astrain D. Massive grid-scale energy storage for next-generation concentrated solar power: A review of the potential emerging concepts. Renew Sust Energ Rev 2023;185:113633.
[13] Bouckaert S, et al. Net zero by 2050-a roadmap for the global energy 773 sector. Paris: International Energy Agency; 2021.
[14] IRENA. Renewable Power Generation Costs in 2022. Abu Dhabi: International Renewable Energy Agency; 2023.
[15] Ren L, Xin Zhao, Zhang Y, Li Y. The economic performance of concentrated solar power industry in China. J Clean Prod 2018;205:799–813.
[16] Quaschning V. Technical and economical system comparison of photovoltaic and concentrating solar thermal power systems depending on annual global irradiation. Sol Energy 2004;77:171–8.
[17] Desideri U, Zepparelli F, Morettini V, Garroni E. Comparative analysis of concentrating solar power and photovoltaic technologies: Technical and environmental evaluations. Appl Energy 2013;102:765–84.
[18] Desideri U, Campana PE. Analysis and comparison between a concentrating solar and a photovoltaic power plant. Appl Energy 2014;113:422–33.
[19] Hernández-Moro J, Martínez-Duart JM. Analytical model for solar PV and CSP electricity costs: Present LCOE values and their future evolution. Renew Sust Energ Rev 2013;20:119–32.
[20] Pietzcker RC, Stetter D, Manger S, Luderer G. Using the sun to decarbonize the power sector: The economic potential of photovoltaics and concentrating solar power. Appl Energy 2014;135:704–20.
[21] Khan J, Arsalan MH. Solar power technologies for sustainable electricity generation – A review. Renew Sust Energ Rev 2016;55:414–25.
[22] Awan AB, Zubair M, Praveen RP, Bhatti AR. Design and comparative analysis of photovoltaic and parabolic trough based CSP plants. Sol Energy 2019;183:551–65.
[23] Awan AB, Zubair M, Chandra Mouli KVV. Design, optimization and performance comparison of solar tower and photovoltaic power plants. Energy 2020;199:117450.
[24] Awan AB, Zubair M, Memon ZA, Ghalleb N, Tlili I. Comparative analysis of dish Stirling engine and photovoltaic technologies: Energy and economic perspective. Sustain Energy Technol Assess 2021;44:101028.
[25] Pfenninger S, Gauché P, Lilliestam J, Damerau K, Wagner F, Patt A. Potential for concentrating solar power to provide baseload and dispatchable power. Nat Clim Chang 2014;4:689–92.
[26] Chung-Ling Chien J, Lior N. Concentrating solar thermal power as a viable alternative in China's electricity supply. Energy Policy 2011;39:7622–36.
[27] Pfenninger S, Keirstead J. Comparing concentrating solar and nuclear power as baseload providers using the example of South Africa. Energy 2015;87:303–14.
[28] Li M, Lenzen M, Yousefzadeh M, Ximenes FA. The roles of biomass and CSP in a 100 % renewable electricity supply in Australia. Biomass Bioenergy 2020;143:105802.
[29] Parrado C, Girard A, Simon F, Fuentealba E. 2050 LCOE (Levelized Cost of Energy) projection for a hybrid PV (photovoltaic)-CSP (concentrated solar power) plant in the Atacama Desert, Chile. Energy 2016;94:422–30.
[30] Starke AR, Cardemil JM, Escobar RA, Colle S. Assessing the performance of hybrid CSP + PV plants in northern Chile. Sol Energy 2016;138:88–97.
[31] Du E, Zhang N, Hodge B-M, Wang Q, Kang C, Kroposki B, et al. The role of concentrating solar power towards high renewable energy penetrated power systems. IEEE Trans Power Syst 2018;33:6630–41.
[32] Yang S, Lao K—W, Hui H, Chen Y.. Secure distributed control for demand response in power systems against deception cyber-attacks with arbitrary patterns. IEEE Trans Power Syst 2024:1–12.
[33] Yang S, Lao K—W, Chen Y, Hui H.. Resilient distributed control against false data injection attacks for demand response. IEEE Trans Power Syst 2024;39:2837–53.
[34] China Electricity Council. China Electric Power Statistic Yearbook 2020. 2020.
[35] National Energy Administration. The National Energy Administration released the electricity consumption of the whole society in 2012. 2013.
[36] National Energy Administration. The National Energy Administration released the electricity consumption of the whole society in 2013. 2014.
[37] National Energy Administration. The National Energy Administration released the electricity consumption of the whole society in 2014:2015.
[38] National Energy Administration. The National Energy Administration released the electricity consumption of the whole society in 2015. 2016.
[39] China Solar Thermal Alliance. Solar Thermal Power Generation Professional Committee of China Renewable Energy Society. China Solar Thermal Power Generation Industry Blue Book 2024;2023.
[40] CSPPLAZA. The total installed capacity exceeds 4GW! Summary of CSP projects under construction/to be developed in my country. https://www.cspplaza.com/article-22289-1.html; 2022.
[41] IRENA. Renewable capacity statistics 2016. Abu Dhabi: International Renewable Energy Agency; 2016.
[42] National Development and Reform Commission. Catalogue for the Guidance of the Development of Renewable Energy Industry. 2005.
[43] National Development and Reform Commission. Medium- and Long-term Development Plan for Renewable Energy. 2007.
[44] National Development and Reform Commission. Eleventh Five-Year Plan for Renewable Energy Development. 2008.
[45] CSPPLAZA. The 1 MW tower CSP demonstration power station project in Yanqing, China, successfully generated electricity. https://www.cspplaza.com/article-586-1.html; 2024.
[46] National Energy Administration. Notice on Organizing the Construction of Solar Thermal Power Generation Demonstration Projects. 2015.
[47] National Development and Reform Commission. Notice on the Benchmark Feed-in Tariff Policy for Solar Thermal Power Generation. 2016.
[48] National Development and Reform Commission. Notice on Matters Concerning the 2021 New Energy Feed-in Tariff Policy. 2021.

[49] National Energy Administration. Notice on matters related to promoting the large-scale development of CSP. 2023.
[50] Ministry of Ecology and Environment. Emission standard of air pollutants for thermal power plants. 2011.
[51] Ministry of Ecology and Environment. National Development and Reform Commission, National Energy Administration. Action Plan for Upgrading and Transforming Coal-fired Power Plants for Energy Conservation and Emission Reduction (2014–2020). 2014.
[52] National Energy Administration. Action Plan for Clean and Efficient Utilization of Coal (2015–2020). 2015.
[53] National Development and Reform Commission. National Energy Administration. Notice on Promoting the Orderly Development of Coal Power in China. 2016.
[54] Ministry of Ecology and Environment. National Development and Reform Commission, Ministry of Industry and Information Technology, Ministry of Housing and Urban-Rural Development, Ministry of Transport, Ministry of Agriculture and Rural Affairs. In: National Energy Administration. Implementation plan for synergies in pollution reduction and carbon reduction; 2022.
[55] National Development and Reform Commission. National Energy Administration. In: Notice on carrying out the transformation and upgrading of coal-fired power units across the country; 2021.
[56] Ministry of Ecology and Environment. Principles for examination and approval of environmental impact assessment documents for thermal power construction projects. 2022.
[57] Silvi C. The pioneering work on linear Fresnel reflector concentrators (LFCs) in Italy. In: The 15th International Symposium on Solar Thermal Concentrating Technologies. Berlin, Germany; 2009.
[58] European Academices Science Advisory Council (EASAC). Concentrating Solar Power: Its potential contribution to a sustainable energy future. 2011.
[59] Baharoon DA, Rahman HA, Omar WZW, Fadhl SO. Historical development of concentrating solar power technologies to generate clean electricity efficiently – A review. Renew Sust Energ Rev 2015;41:996–1027.
[60] IRENA. Renewable energy technologies cost analysis series: concentrating solar power. Abu Dhabi: International Renewable Energy Agency; 2012.
[61] Government of Spain. National Energy Action Plan Renewables of Spain (PANER) 2011–2020. Tourism and Commerce, Government of Spain: Ministry of Industry; 2010.
[62] Government of Spain. National Energy Action Plan Renewables of Spain (PANER) 2005–2010. Tourism and Commerce, Government of Spain: Ministry of Industry; 2004.
[63] Radosevich LG. Final report on the power production phase of the 10 MW/sub e/ Solar Thermal Central Receiver Pilot Plant. Sandia National Lab. Livermore, CA (United States): (SNL-CA); 1988.
[64] Pool S, Coggin JDP. Fulfilling the promise of concentrating solar power. Center for American Progress; 2013.
[65] NREL. Archimede solar thermal plant: parabolic trough technology. 2013.
[66] CMS. CMS Expert Guide to renewable energy law and regulation Renewable energy law and regulation in Morocco. 2018.
[67] Accounts C. Report on the compensation system in Morocco Diagnosis and reform proposals. Rabat. January 2014.
[68] Eberhard A, Leigland J, Kolker J. South Africa's renewable energy IPP procurement program. World Bank Publications; 2014.
[69] Musango JK, Brent AC. A roadmap framework for solar aided power generation in South Africa. J Energy in Southern Africa 2015;26:2–15.
[70] The United Arab Emirates' Government portal (UAE). UAE Energy Strategy 2050 2023.
[71] Macrotrends. Crude Oil Prices - 70 Year Historical Chart. https://www.macrotrends.net/1369/crude-oil-price-history-chart; 2024.
[72] U.S. Department of Energy. Loan Guarantee. Program. 2009.
[73] U.S. Department of Energy. Loan Guarantee Program for Solar Projects. 2012.
[74] U.S. Congress. Consolidated Appropriations Act of 2015. 2015.
[75] Government of Morocco. Phaseout of Fossil Fuel Subsidies. Moroccan Agency for Solar Energy (MASEN). 2014.
[76] Ministry of Energy, Chile. Renewable Power Supply Auctions. 2014.
[77] Government of South Africa. Renewable Energy Independent Power Producer Procurement Program (REIPPPP). 2018.
[78] Ministry of Energy. Government of Chile. An Energy Agenda Transformative for a Sustainable Future. 2022.
[79] Ministry of Energy. Government of Chile. Actions for an accelerated decarbonisation of the electricity sector. 2022.
[80] Yeh S, Rubin ES. A centurial history of technological change and learning curves for pulverized coal-fired utility boilers. Energy 2007;32:1996–2005.
[81] Zhang Z, Zhou R, Ge X, Zhang J, Wu X. Perspectives for 700 °C ultra-supercritical power generation: Thermal safety of high-temperature heating surfaces. Energy 2020;190:116411.
[82] Fukuda M. Advanced USC technology development in Japan. Materials for ultra-supercritical and advanced ultra-supercritical power plants. Elsevier; 2017. p. 733–54.
[83] Bugge J, Kjær S, Blum R. High-efficiency coal-fired power plants development and perspectives. Energy 2006;31:1437–45.
[84] Chang S, Zhuo J, Meng S, Qin S, Yao Q. Clean coal technologies in china: Current status and future perspectives. Engineering 2016;2:447–59.
[85] Tong D, Zhang Q, Liu F, Geng G, Zheng Y, Xue T, et al. Current emissions and future mitigation pathways of coal-fired power plants in china from 2010 to 2030. Environ Sci Technol 2018;52:12905–14.
[86] Xu C, Wang Z, Li X, Sun F. Energy and exergy analysis of solar power tower plants. Appl Therm Eng 2011;31:3904–13.
[87] Zhang Q, Wang Z, Du X, Yu G, Wu H. Dynamic simulation of steam generation system in solar tower power plant. Renew Energy 2019;135:866–76.
[88] Yao Z, Wang Z, Lu Z, Wei X. Modeling and simulation of the pioneer 1 MW solar thermal central receiver system in China. Renew Energy 2009;34:2437–46.
[89] Liu T, Bai Z, Zheng Z, Liu Q, Lei J, Sui J, et al. 100 kW_e power generation pilot plant with a solar thermochemical process: design, modeling, construction, and testing. Appl Energy 2019;251:113217.
[90] Yao L, Xiao X, Wang Y, Yao X, Ma Z. Dynamic modeling and hierarchical control of a concentrated solar power plant with direct molten salt storage. Energy 2022;252:123999.
[91] Yao L, Wang Y, Xiao X. Concentrated solar power plant modeling for power system studies. IEEE Trans Power Syst 2024;39:4252–63.
[92] Dongfang Turbine Co.,Ltd. of Dongfang Electric Corporation. Product structure, new energy, solar thermal power generation. https://www.dfstw.com/products/p1.aspx?articleid=2790.
[93] Shanghai Electric Power Generation Equipment Co.,Ltd. Turbine Plant. Project case, Yumen Xinneng solar thermal power generation project. https://www.shanghai-electric.com/listed/c/2019-09-17/536071.shtml.
[94] Kocaarslan İ, Çam E, Tiryaki H. A fuzzy logic controller application for thermal power plants. Energy Convers Manag 2006;47:442–58.
[95] You X, Dian S, Liu K, Guo B, Xiang G, Zhu Y. Command filter-based adaptive fuzzy finite-time tracking control for uncertain fractional-order nonlinear systems. IEEE Trans Fuzzy Syst 2022;31:226–40.
[96] Garduno-Ramirez R, Lee KY. Wide range operation of a power unit via feedforward fuzzy control [thermal power plants]. IEEE Trans Energy Convers 2000;15:421–6.
[97] Basu S, Debnath AK. Power plant instrumentation and control handbook: A guide to thermal power plants. Academic press; 2014.
[98] National Energy Administration. National Energy Administration's announcement on organizing solar thermal power generation demonstration projects Construction Notice. 2015.
[99] Ministry of Natural Resources of the People's Republic of China. Explanation of land quotas for construction of thermal power plants. 2008.
[100] Arán Carrión J, Espín Estrella A, Aznar Dols F, Zamorano Toro M, Rodríguez M, Ramos Ridao A. Environmental decision-support systems for evaluating the carrying capacity of land areas: Optimal site selection for grid-connected photovoltaic power plants. Renew Sust Energ Rev 2008;12:2358–80.
[101] Aly A, Jensen SS, Pedersen AB. Solar power potential of Tanzania: Identifying CSP and PV hot spots through a GIS multicriteria decision making analysis. Renew Energy 2017;113:159–75.
[102] Yushchenko A, de Bono A, Chatenoux B, Kumar Patel M, Ray N. GIS-based assessment of photovoltaic (PV) and concentrated solar power (CSP) generation potential in West Africa. Renew Sust Energ Rev 2018;81:2088–103.
[103] Ahmad M, Zeeshan M. Validation of weather reanalysis datasets and geospatial and techno-economic viability and potential assessment of concentrated solar power plants. Energy Convers Manag 2022;256:115366.
[104] Jbaihi O, Ouchani F, Alami Merrouni A, Cherkaoui M, Ghennioui A, Maaroufi M. An AHP-GIS based site suitability analysis for integrating large-scale hybrid CSP + PV plants in Morocco: An approach to address the intermittency of solar energy. J Clean Prod 2022;369:133250.
[105] Brewer J, Ames DP, Solan D, Lee R, Carlisle J. Using GIS analytics and social preference data to evaluate utility-scale solar power site suitability. Renew Energy 2015;81:825–36.
[106] He G, Kammen DM. Where, when and how much solar is available? A provincial-scale solar resource assessment for China. Renew Energy 2016;85:74–82.
[107] Chen F, Yang Q, Zheng N, Wang Y, Huang J, Xing L, et al. Assessment of concentrated solar power generation potential in China based on Geographic Information System (GIS). Appl Energy 2022;315:119045.
[108] Anwarzai MA, Nagasaka K. Utility-scale implementable potential of wind and solar energies for Afghanistan using GIS multi-criteria decision analysis. Renew Sust Energ Rev 2017;71:150–60.
[109] Aly A, Bernardos A, Fernandez-Peruchena CM, Jensen SS, Pedersen AB. Is concentrated solar power (csp) a feasible option for sub-saharan africa?: Investigating the techno-economic feasibility of CSP in Tanzania. Renew Energy 2019;135:1224–40.
[110] Romero-Ramos JA, Gil JD, Cardemil JM, Escobar RA, Arias I, Pérez-García M. A GIS-AHP approach for determining the potential of solar energy to meet the thermal demand in southeastern Spain productive enclaves. Renew Sust Energ Rev 2023;176:113205.
[111] Haddad B, Díaz-Cuevas P, Ferreira P, Djebli A, Pérez JP. Mapping concentrated solar power site suitability in Algeria. Renew Energy 2021;168:838–53.
[112] Watson JJW, Hudson MD. Regional Scale wind farm and solar farm suitability assessment using GIS-assisted multi-criteria evaluation. Landsc Urban Plan 2015;138:20–31.
[113] Sun L, Jiang Y, Guo Q, Ji L, Xie Y, Qiao Q, et al. A GIS-based multi-criteria decision making method for the potential assessment and suitable sites selection of PV and CSP plants. Resour Conserv Recycl 2021;168:105306.
[114] Qaisrani MA, Wei J, Khan LA. Potential and transition of concentrated solar power: A case study of China. Sustain Energy Technol Assess 2021;44:101052.
[115] Zhang Y, Ren J, Pu Y, Wang P. Solar energy potential assessment: A framework to integrate geographic, technological, and economic indices for a potential analysis. Renew Energy 2020;149:577–86.
[116] Forman EH, Gass SI. The analytic hierarchy process—An exposition. Oper Res 2001;49:469–86.

[117] Fabianek P, Will C, Wolff S, Madlener R. Green and regional? A multi-criteria assessment framework for the provision of green electricity for electric vehicles in Germany. Transp Res Part D: Transp Environ 2020;87:102504.
[118] Saaty TL, Peniwati K. Group decision making: drawing out and reconciling differences. Pittsburgh: RWS public; 2013.
[119] National Energy Administration. Specification for acceptance of thermal power engineering reached the standard and put into production. 2012.
[120] Xu J, Song X, Wu Y, Zeng Z. GIS-modeling based coal-fired power plant site identification and selection. Appl Energy 2015;159:520–39.
[121] Janke JR. Multicriteria GIS modeling of wind and solar farms in Colorado. Renew Energy 2010;35:2228–34.
[122] Noorollahi Y, Ghenaatpisheh Senani A, Fadaei A, Simaee M, Moltames R. A framework for GIS-based site selection and technical potential evaluation of PV solar farm using Fuzzy-Boolean logic and AHP multi-criteria decision-making approach. Renew Energy 2022;186:89–104.
[123] Rios R, Duarte S. Selection of ideal sites for the development of large-scale solar photovoltaic projects through Analytical Hierarchical Process – Geographic information systems (AHP-GIS) in Peru. Renew Sust Energ Rev 2021;149:111310.
[124] Günen MA. A comprehensive framework based on GIS-AHP for the installation of solar PV farms in Kahramanmaraş. Turkey Renew Energy 2021;178:212–25.
[125] Ruiz HS, Sunarso A, Ibrahim-Bathis K, Murti SA, Budiarto I. GIS-AHP Multi Criteria Decision Analysis for the optimal location of solar energy plants at Indonesia. Energy Rep 2020;6:3249–63.
[126] Giamalaki M, Tsoutsos T. Sustainable siting of solar power installations in Mediterranean using a GIS/AHP approach. Renew Energy 2019;141:64–75.
[127] Rediske G, Siluk JCM, Michels L, Rigo PD, Rosa CB, Cugler G. Multi-criteria decision-making model for assessment of large photovoltaic farms in Brazil. Energy 2020;197:117167.
[128] Alami Merrouni A, Elwali Elalaoui F, Mezrhab A, Mezrhab A, Ghennioui A. Large scale PV sites selection by combining GIS and Analytical Hierarchy Process. Case study: Eastern Morocco Renew Energy 2018;119:863–73.
[129] Asakereh A, Soleymani M, Sheikhdavoodi MJ. A GIS-based Fuzzy-AHP method for the evaluation of solar farms locations: Case study in Khuzestan province. Iran Solar Energy 2017;155:342–53.
[130] Al Garni HZ, Awasthi A. Solar PV power plant site selection using a GIS-AHP based approach with application in Saudi Arabia. Appl Energy 2017;206:1225–40.
[131] Sindhu S, Nehra V, Luthra S. Investigation of feasibility study of solar farms deployment using hybrid AHP-TOPSIS analysis: Case study of India. Renew Sust Energ Rev 2017;73:496–511.
[132] Uyan M. GIS-based solar farms site selection using analytic hierarchy process (AHP) in Karapinar region. Konya/Turkey Renew Sustain Energy Rev 2013;28:11–7.
[133] Alami Merrouni A, Elwali Elalaoui F, Ghennioui A, Mezrhab A, Mezrhab A. A GIS-AHP combination for the sites assessment of large-scale CSP plants with dry and wet cooling systems. Case study: Eastern Morocco Solar Energy 2018;166:2–12.
[134] Ziuku S, Seyitini L, Mapurisa B, Chikodzi D, van Kuijk K. Potential of Concentrated Solar Power (CSP) in Zimbabwe. Energy for Sustainable Development 2014;23:220–7.
[135] Hermann S, Miketa A, Fichaux N. Estimating the renewable energy potential in Africa: A GIS-based approach. Abu Dhabi: International Renewable Energy Agency; 2014.
[136] Ju X, Xu C, Hu Y, Han X, Wei G, Du X. A review on the development of photovoltaic/concentrated solar power (PV-CSP) hybrid systems. Sol Energy Mater Sol Cells 2017;161:305–27.
[137] Branker K, Pathak MJM, Pearce JM. A review of solar photovoltaic levelized cost of electricity. Renew Sust Energ Rev 2011;15:4470–82.
[138] Zhao Z-Y, Chen Y-L, Thomson JD. Levelized cost of energy modeling for concentrated solar power projects: A China study. Energy 2017;120:117–27.
[139] Ouyang X, Lin B. Levelized cost of electricity (LCOE) of renewable energies and required subsidies in China. Energy Policy 2014;70:64–73.
[140] Zurita A, Mata-Torres C, Valenzuela C, Felbol C, Cardemil JM, Guzmán AM, et al. Techno-economic evaluation of a hybrid CSP + PV plant integrated with thermal energy storage and a large-scale battery energy storage system for base generation. Sol Energy 2018;173:1262–77.
[141] Zurita A, Mata-Torres C, Cardemil JM, Escobar RA. Assessment of time resolution impact on the modeling of a hybrid CSP-PV plant: A case of study in Chile. Sol Energy 2020;202:553–70.
[142] Lei C, Wang Q, Zhou G, Bu S, Zhou N, Lin T, et al. Probabilistic wind power expansion planning of bundled wind-thermal generation system with retrofitted coal-fired plants using load transfer optimization. Int J Electr Power Energy Syst 2023;151:109145.
[143] Li R, Jin X, Yang P, Feng Y, Liu Y, Wang S, et al. Large-scale offshore wind energy integration by wind-thermal bundled power system: A case study of Yangxi. China J Cleaner Pro 2024;435:140601.
[144] China Solar Thermal Alliance. Comprehensive interpretation of the construction and operation of China Power Construction Qinghai Gonghe 50 MW Tower CSP Project. http://www.cnste.org/html/jishu/2020/0909/6918.html.
[145] China Solar Thermal Alliance. The entire construction and operation process of Shouhang Energy Saving Dunhuang 100 MW molten solar thermal power plant. http://www.cnste.org/html/xiangmu/2019/0726/5243.html.
[146] Lu S, Gu W, Xu Y, Dong ZY, Sun L, Zhang H, et al. Unlock the thermal flexibility in integrated energy systems: A robust nodal pricing approach for thermal loads. IEEE Trans on Smart Grid 2023;14:2734–46.
[147] Dong S, Zang T, Zhou B, Luo H, Zhou Y, Xiao X. Robust coordinated resilience enhancement strategy for communication networks of power and thermal cyber-physical systems considering decision-dependent uncertainty. Appl Energy 2024;368:123494.
[148] Tian H, Chen M, Liang G, Xiao X. A single-phase transformerless common-ground type pv inverter with active power decoupling. IEEE Trans Ind Electron 2023;70:3762–72.
[149] Jimenez-Navarro J-P, Kavvadias K, Filippidou F, Pavičević M, Quoilin S. Coupling the heating and power sectors: The role of centralized combined heat and power plants and district heat in a European decarbonised power system. Appl Energy 2020;270:115134.
[150] He G, Chen Q, Kang C, Xia Q. Optimal offering strategy for concentrating solar power plants in joint energy, reserve and regulation markets. IEEE Trans Sustain Energy 2016;7:1245–54.
[151] Yao H, Xiang Y, Gu C, Liu J. Peer-to-Peer coupled trading of energy and carbon emission allowance: a stochastic game-theoretic approach. IEEE Internet Things J 2024;11:24364–75.
[152] Du E, Zhang N, Hodge B-M, Wang Q, Lu Z, Kang C, et al. Operation of a high renewable penetrated power system with CSP plants: A look-ahead stochastic unit commitment model. IEEE Trans Power Syst 2018;34:140–51.
[153] Jiang Y, Ren Z, Li W. Committed carbon emission operation region for integrated energy systems: concepts and analyses. IEEE Trans Sustain Energy 2024;15:1194–209.
[154] Yang L, Li H, Zhang H, Wu Q, Cao X. Stochastic-Distributionally robust frequency-constrained optimal planning for an isolated microgrid. IEEE Trans Sustain Energy 2024:1–15.
[155] Fang Y, Zhao S. Look-ahead bidding strategy for concentrating solar power plants with wind farms. Energy 2020;203:117895.